pharmaceutics

MDPI

Article

Dual Targeting Ligands—Histamine H_3 Receptor Ligands with Monoamine Oxidase B Inhibitory Activity—In Vitro and In Vivo Evaluation

Dorota Łażewska [1,*], Agata Siwek [2], Agnieszka Olejarz-Maciej [1], Agata Doroz-Płonka [1], Anna Wiktorowska-Owczarek [3], Marta Jóźwiak-Bębenista [3], David Reiner-Link [4], Annika Frank [4], Wioletta Sromek-Trzaskowska [1], Ewelina Honkisz-Orzechowska [1], Ewelina Królicka [1], Holger Stark [4], Marek Wieczorek [5], Waldemar Wagner [6,7], Katarzyna Kieć-Kononowicz [1] and Anna Stasiak [6,*]

1 Department of Technology and Biotechnology of Drugs, Faculty of Pharmacy, Jagiellonian University Medical College in Kraków, Medyczna 9 Str., 30-688 Kraków, Poland
2 Department of Pharmacobiology, Faculty of Pharmacy, Jagiellonian University Medical College in Kraków, Medyczna 9 Str., 30-688 Kraków, Poland
3 Department of Pharmacology and Toxicology, Medical University of Lodz, Żeligowskiego 7/9 Str., 90-752 Łódź, Poland
4 Institute of Pharmaceutical and Medicinal Chemistry, Heinrich Heine University Düsseldorf, Universitaetsstr. 1, 40225 Düsseldorf, Germany
5 Department of Neurobiology, Faculty of Biology and Environmental Protection, University of Lodz, Pomorska 141/143 Str., 90-236 Łódź, Poland
6 Department of Hormone Biochemistry, Medical University of Lodz, Żeligowskiego 7/9 Str., 90-752 Łódź, Poland
7 Laboratory of Cellular Immunology, Institute of Medical Biology of Polish Academy of Sciences, 106 Lodowa Str., 93-232 Łódź, Poland
* Correspondence: dorota.lazewska@uj.edu.pl (D.Ł.); anna.stasiak@umed.lodz.pl (A.S.)

check for updates

Citation: Łażewska, D.; Siwek, A.; Olejarz-Maciej, A.; Doroz-Płonka, A.; Wiktorowska-Owczarek, A.; Jóźwiak-Bębenista, M.; Reiner-Link, D.; Frank, A.; Sromek-Trzaskowska, W.; Honkisz-Orzechowska, E.; et al. Dual Targeting Ligands—Histamine H_3 Receptor Ligands with Monoamine Oxidase B Inhibitory Activity—In Vitro and In Vivo Evaluation. *Pharmaceutics* **2022**, *14*, 2187. https://doi.org/10.3390/pharmaceutics14102187

Academic Editor: Tatiana B. Tennikova

Received: 12 September 2022
Accepted: 9 October 2022
Published: 13 October 2022

Abstract: The clinical symptoms of Parkinson's disease (PD) appear when dopamine (DA) concentrations in the striatum drops to around 20%. Simultaneous inhibitory effects on histamine H_3 receptor (H_3R) and MAO B can increase DA levels in the brain. A series of compounds was designed and tested in vitro for human H_3R (hH_3R) affinity and inhibitory activity to human MAO B (hMAO B). Results showed different activity of the compounds towards the two biological targets. Most compounds had poor affinity for hH_3R (K_i > 500 nM), but very good inhibitory potency for hMAO B (IC_{50} < 50 nM). After further in vitro testing (modality of MAO B inhibition, permeability in PAMPA assay, cytotoxicity on human astrocyte cell lines), the most promising dual-acting ligand, 1-(3-(4-(tert-butyl)phenoxy)propyl)-2-methylpyrrolidine (**13**: hH_3R: K_i = 25 nM; hMAO B IC_{50} = 4 nM) was selected for in vivo evaluation. Studies in rats of compound **13**, in a dose of 3 mg/kg of body mass, confirmed its antagonistic effects for H_3R (decline in food and a water consumption), decline in MAO B activity (>90%) in rat cerebral cortex (CTX), and an increase in DA content in CTX and striatum. Moreover, compound **13** caused a slight increase in noradrenaline, but a reduction in serotonin concentration in CTX. Thus, compound **13** is a promising dual-active ligand for the potential treatment of PD although further studies are needed to confirm this.

Keywords: histamine H_3 receptor; histamine H_3 receptor ligand; monoamine oxidase B (MAO B); MAO B inhibitor; dual-target ligands; pitolisant; in vivo studies

1. Introduction

Parkinson's disease (PD) is characterized by a progressive loss of dopaminergic neurons in the *substantia nigra* and the accumulation of misfolded and aggregated α-synuclein named Lewy bodies. All of this leads to a decrease in the level of dopamine (DA) in the *striatum* causing memory deficits and also problems with moving. However, it should be remembered that a decline in DA levels is a normal process of ageing and it could

be reduced by 40–50% of the beginning amount at the age of 60. However, the motor symptoms of PD (such as bradykinesia, tremor and stiffness) are observed when DA concentration is diminished by 80% of the initial volume. Compensation for DA shortage in the brain could be achieved among others by activation of DA receptors by the precursor of DA—*levodopa*, and DA agonists (e.g., *bromocriptine*, *rotigotine*), and by blocking of enzymes metabolizing DA such as monoamine oxidase B (MAO B) inhibitors (e.g., *selegiline*, *rasagiline*), or catechol-*O*-methyltransferase (COMT) inhibitors (e.g., *entacapone*, *tolcapone*). Moreover, blockade of histamine H_3 receptors (H_3R) could increase the level of DA in the brain. Histamine H_3R are presynaptic receptors mainly distributed in the central nervous system, especially in the region connected with memory and learning. As heteroreceptors, they are located at the endings of non-histaminergic neurons (e.g., DA, acetylcholine, noradrenaline, serotonin). Deactivation of these receptors leads to enhanced release of the proper neurotransmitters including DA. PD is neurodegenerative disorder with a complicated etiology, and it is currently believed that only the use of drugs acting on several biological targets simultaneously can be effective in its treatment [1]. Thus, the search for multi-target drugs has developed in the last few years [1,2]. This novel strategy in drug design and development focuses on a combination of classical targets (e.g., MAO B inhibition) with new targets e.g., adenosine A_{2A} receptor blockade [3] or histamine H_3R inhibition [4–7]. The concept of dual target ligands (DTL) linking blockade of MAO B with inhibition of H_3R emerged a few years ago when preliminary screening for inhibitory activity toward human MAO B (hMAO B) showed promising inhibition of this enzyme by H_3R ligands: ciproxifan (IC_{50} = 2 μM; Figure 1) and DL77 (IC_{50} = 19 nM; Figure 1) [6,8]. Thereafter, designed molecules were created as hybrids combining elements responsible for interaction with H_3R (piperidine propyloxyphenyl element), and an MAO B motif e.g., a propargylamine moiety (**1**&**2**; Figure 1). These compounds showed stronger affinity for human H_3R (hH_3R) than hMAO B inhibitory activity. By contrast, some analogues of DL77 synthesized by our group with 4-*tert*-pentylphenyl moiety showed higher inhibitory activity for hMAO B than affinity for hH_3R, e.g., compound **3** (hH_3R K_i = 63 nM; hMAO B IC_{50} = 4.5 nM; Figure 1) [6].

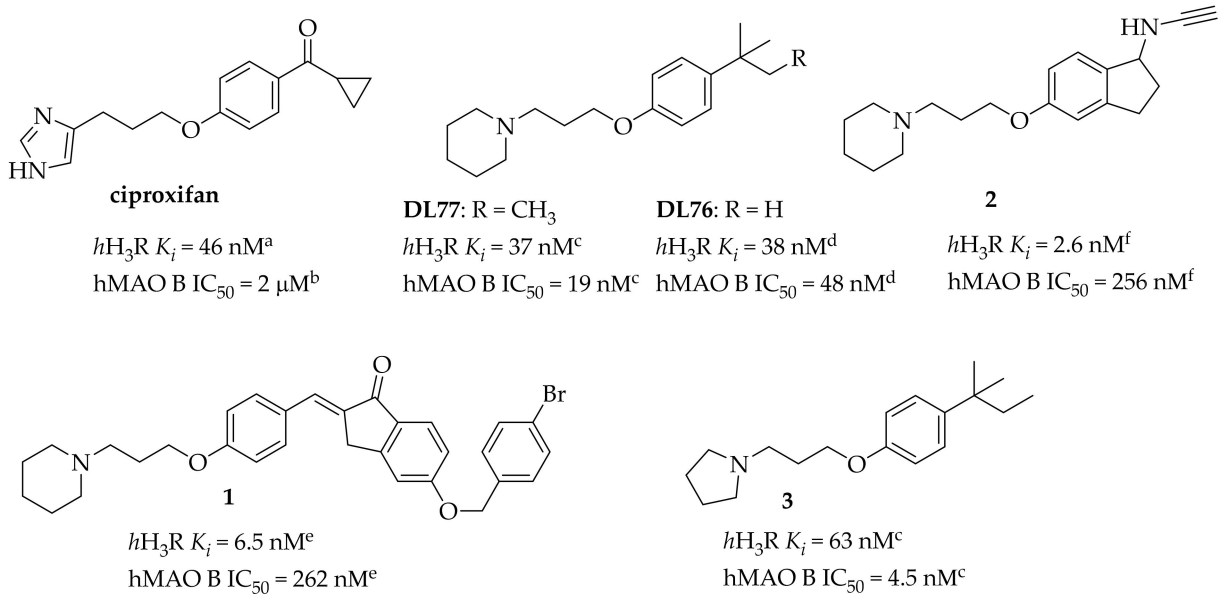

Figure 1. Structures of DTL–histamine H_3 receptor ligands with MAO B inhibitory activity. [a]: data from Ref. [9]; [b]: from [8]; [c]: from [6]; [d]: from [7]; [e]: from [4]; [f]: from [5].

Recently, we described DTL with the 4-*tert*-butylphenyl scaffold as hH_3R ligands and hMAO B inhibitors [7]. This study is a continuation of the previous work with further structural modification of the lead compound DL76 (dual target activity: hH_3R K_i = 38 nM,

hMAO B IC_{50} = 48 nM [7]) (Figure 1). Three types of modifications were introduced in the lead structure (Figure 2). All compounds obtained were tested for affinity to hH_3R stably expressed in CHO or HEK293 cells. The inhibitory activity against hMAO B was evaluated by fluorometric MAO assay. For the two most potent hMAO B inhibitors (**9** and **13**; Table 1), the modality of hMAO B inhibition was assessed as well as an ability to cross the blood–brain barrier by using artificial membrane permeation assay (PAMPA). Next, the compound **13** was selected for further in vivo tests. The assessment concerned the effects of **13** on the feeding behavior of rats after its repeated peripheral injections and the influence on MAO A and B, and histamine *N*-methyltransferase (HNMT) activities, as well as cerebral catecholamine and serotonin concentrations.

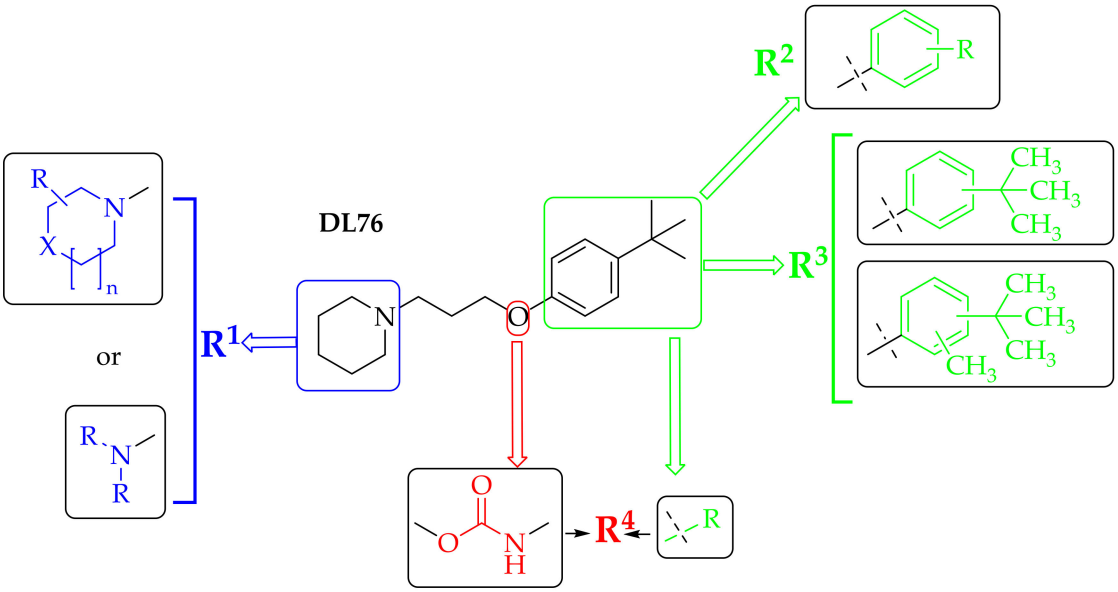

Figure 2. General structural modifications of **DL76**.

Table 1. In vitro affinities for human histamine H_3 receptor and human MAO B inhibitory activities of the target compounds **4**–**17**.

Compound	Structure	hH_3R [a,b] K_i [nM] ± SEM [a] or K_i [nM] [95%CI] [b] (% Inh.) [c]	hMAO B [d] IC_{50} [nM] (% of Inh.) [e]
DL76	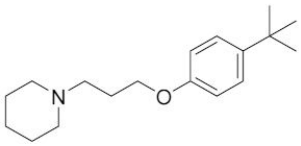	57.5 ± 6.4 [a] 38 [8; 181] [b]	48 ± 15
	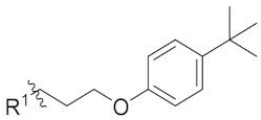		
	R^1		
4		(24%) [c]	19 ± 2
5		484 ± 15 [a]	9 ± 0

Table 1. *Cont.*

Compound	Structure	*h*H$_3$R [a,b] K_i [nM] ± SEM [a] or K_i [nM] [95%CI] [b] (% Inh.) [c]	hMAO B [d] IC$_{50}$ [nM] (% of Inh.) [e]
6		900 ± 75 [a]	6 ± 1
9	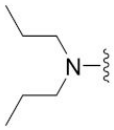	323 ± 73 [a]	2 ± 0
10 [f]	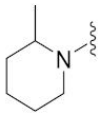	69 [b,f] [49; 96]	11 ± 1[f]
11	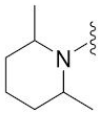	97 ± 3 [a]	9 ± 1
12 [f]		371 [b,f] [136; 1009]	2.7 ± 0.4 [f]
7		(32%) [c]	15 ± 4
8	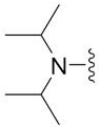	(8%) [c]	37 ± 6
13		25 ± 9 [a]	4.0 ± 0.3
14	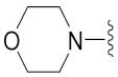	(11%) [c]	192 ± 14
15		(0%) [c]	665 ± 118
16	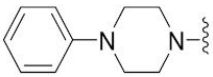	535 ± 41 [a]	(14%) [e]
17	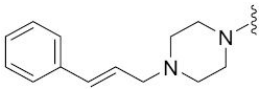	(0%) [c]	(7%) [e]

[a]: [^{3}H]N^α-Methylhistamine-binding assay in CHO-K1 cells stably expressing the *h*H$_3$R; mean value ± SEM of three independent experiments. [b]: [^{3}H]N^α-Methylhistamine-binding assay in HEK293 cells stably expressing the *h*H$_3$R; mean value within the 95% confidence interval (CI) of three independent experiments. [c]: % of radioligand inhibition at *h*H$_3$R (in CHO K1 cells) at 1 μM in two independent experiments, each as triplate; mean value. [d] fluorometric MAO assay; mean value ± SEM of 2–4 independent experiments. [e]: % of inhibition at 1 μM; mean values of two independent experiments. [f]: data from Ref. [7].

2. Materials and Methods

2.1. Synthesis of Compounds

This study is a continuation of the previous work and includes further structural modification of the lead compound DL76 (dual target activity: hH_3R K_i = 38 nM, hMAO B IC_{50} = 48 nM [7]) (Figure 1). The designed structural modification included: (a) change of the piperidine ring for other amines (cyclic or dialkyl), (b) change of a position or the kind of *tert*-butyl substituent, and (c) change of an ether linker for a carbamate linker.

All designed modifications are shown in Figure 2 and structures are collected in Table S1 (Supplementary Materials S1).

Reagents and solvents were obtained from commercial suppliers and used without further purification. Reactions were conducted in the air atmosphere and monitored by thin layer chromatography (Merck silica gel 60 F254 plates). The spot visualization was achieved with UV lamp and Dragendorff's reagent (solvent system: methylene chloride: methanol 9:1 or 1:1). Purity of compounds was confirmed by NMR spectra (^{1}H and ^{13}C) in DMSO-d_6 using Mercury 300 MHz PFG spectrometer (Varian, Palo Alto, CA, USA) or FT-NMR 500 MHz spectrometer (Joel Ltd., Akishima, Tokyo, Japan). The chemical shifts (δ) are reported in relation to tetramethylsilane (TMS) and the coupling constants (J) are expressed in Hz. The multiplicity of each peak is reported as: s, singlet; d, doublet; t, triplet; q, quartet; quin, quintet; m, multiplet; br, broad; def, deformed. Mass spectra (LC/MS) were performed on Waters TQ Detector Mass Spectrometer (Water Corporation, Milford, CT, USA). Retention times (t_R) are given in minutes. UPLC/MS analysis confirmed purity of compounds ≥97% (except **25**: 93%). The elemental analysis (C, h, N) for compounds (**4**–**7**; **9**; **11**; **13**–**16**; **19**; **24**,**25**; **27**–**29**) was performed on Vario EL III Elemental Analyser (Hanau, Germany) and results agreed within 0.5% of the theoretical value.

4-*tert*-Butylphenoxypropyl bromide (Ia) (CAS3245-63-4) was synthesized as described previously [7]. Other phenoxypropylbromides (Ib-Il) were obtained as Ia and all of them (except Ij) are reported in Chemical Abstract Database: 1-(4-(3-bromopropoxy)phenyl)ethan-1-one (Ib): CAS65623-98-5; 1-(3-bromopropoxy)-4-isopropylbenzene (Ic): CAS204979-21-5; 1-(3-bromopropoxy)-4-ethylbenzene (Id): CAS130402-63-0; 1-(3-bromopropoxy)-4-methylbenzene (Ie): CAS16929-24-1; 1-(3-bromopropoxy)-4-flurobenzene (If): CAS1129-78-8; 1-(3-bromopropoxy)-4-chlorobenzene (Ig): CAS27983-04-6; 2-*tert*-butylphenoxypropyl bromide (Ih) CAS414900-40-6; 3-*tert*-butylphenoxypropyl bromide (Ii) CAS1094702-92-7; 2-(3-bromopropoxy)-1-(*tert*-butyl)-3-methylbenzene (Ik) CAS1094273-48-9;1-(3-bromopropoxy)-2-(*tert*-butyl)-4-methylbenzene (Il) CAS1092405-68-6.

Synthesis of below compounds were previously reported:

1-(3-(4-(tert-Butyl)phenoxy)propyl)-2-methylpiperidine hydrogen oxalate (**10**) [7]
1-(3-(4-(tert-Butyl)phenoxy)propyl)-pyrrolidine hydrogen oxalate (**12**) [7]
3-(Piperidin-1-yl)propyl tert-butylcarbamate hydrogen oxalate (**30**) [10]
3-(Piperidin-1-yl)propyl (2,4,4-trimethylpentan-2-yl)carbamate hydrogen oxalate (**31**) [10]
3-(Piperidin-1-yl)propyl (3,3-dimethylbutyl)carbamate hydrogen oxalate (**32**) [10]
General synthetic preparation of compounds **4**–**9**, **11**, **13**–**28**.

To a proper phenoxypropyl bromide (5 mmol) in acetonitrile (25 mL) and in the presence of K_2CO_3 (6 mmol) with the catalytic amount of KI was added a proper amine (5 mmol) and the solution was refluxed from 10 to 72 h. Next, a solid was filtered off and the oily residue was purified by flash chromatography (CH_2Cl_2:CH_3OH, 50:50). The final product was transformed into oxalic acid salt in absolute C_2H_5OH and precipitated $(C_2H_5)_2O$, or the solid was crystallized from C_2H_5OH.

3-(4-(tert-Butyl)phenoxy)-N,N-dimethylpropan-1-amine hydrogen oxalate (**4**)

The title compound was prepared using dimethylamine (0.23 g, 5 mmol) and 4-*tert*-butylphenoxy propyl bromide (1.36 g, 5 mmol). Yield 10%, m.p. 140 dec °C, $C_{15}H_{25}NO \times C_2H_2O_4 \times 0.50\ H_2O$ (MW = 334.42). ^{1}H NMR (500 MHz, DMSO-d_6) δ: 7.25 (d, *J* = 8.6 Hz, 2H), 6.81 (d, *J* = 8.6 Hz, 2H), 3.96 (t, *J* = 6.3 Hz, 2H), 3.16—3.04 (m, 2H), 2.71 (s, 6H), 2.13–1.97 (m, 2H), 1.21 (s, 9H). ^{13}C NMR (126 MHz, DMSO-d_6) δ: 165.2, 156.6, 143.5, 126.6, 114.5, 65.3,

54.7, 42.8, 34.3, 31.9, 24.6. LC-MS: purity 100% t_R = 5.01, (ESI) *m/z* [M + H]$^+$ 236.06. Analysis calculated for $C_{17}H_{28}NO_{5.5}$: C, 61.05; h, 8.37; N, 4.19%. Found: C, 61.22; h, 8.61; N, 4.10%.

3-(4-(tert-Butyl)phenoxy)-N-ethyl-N-methylpropan-1-amine hydrogen oxalate (**5**)

The title compound was prepared using *N*-methylethamine (0.30 g, 5 mmol) and 4-*tert*-butylphenoxy propyl bromide (1.36 g, 5 mmol). Yield 7%, m.p. 131 dec °C, $C_{16}H_{27}NO \times C_2H_2O_4 \times 0.25H_2O$ (MW = 343.94). ^{1}H NMR (500 MHz, DMSO-d$_6$) δ: 7.25 (d, *J* = 8.59 Hz, 2H), 6.81 (d, *J* = 8.59 Hz, 2H), 3.97 (t, *J* = 5.73 Hz, 2H), 2.96–3.21 (m, 4H), 2.68 (s, 3H), 2.11–1.96 (m, 2H), 1.21 (s, 9H), 1.16 (t, *J* = 7.45 Hz, 3H). ^{13}C NMR (126 MHz, DMSO-d$_6$) δ: 165.3, 156.6, 143.5, 126.6, 114.5, 65.4, 52.3, 50.4, 39.2, 34.3, 31.9, 24.2, 9.5. LC-MS: purity 100% t_R = 5.21, (ESI) *m/z* [M + H]$^+$ 250.15. Analysis calculated for $C_{18}H_{29.5}NO_{5.25}$: C, 62.85; h, 8.40; N, 4.07%. Found: C, 62.80; h, 8.77; N, 4.00%.

3-(4-(tert-Butyl)phenoxy)-N-isopropyl-N-methylpropan-1-amine hydrogen oxalate (**6**)

The title compound was prepared using *N*-methylpropan-2-amine (0.37 g, 5 mmol) and 4-*tert*-butylphenoxy propyl bromide (1.36 g, 5 mmol). Yield 3%, m.p. 128 dec °C, $C_{17}H_{29}NO \times C_2H_2O_4 \times 0.5H_2O$ (MW = 362.47). ^{1}H NMR (500 MHz, DMSO-d$_6$) δ: 7.25 (d, *J* = 8.59 Hz, 2H), 6.82 (d, *J* = 9.17 Hz, 2H), 3.97 (t, *J* = 6.01 Hz, 2H), 3.42–3.55 (m, 1H), 2.97–3.19 (m, 2H), 2.54–2.65 (m, 3H), 2.05 (dd, *J* = 6.59, 8.88 Hz, 2H), 1.21 (s, 9H), 1.17 (d, *J* = 6.30 Hz, 6H). ^{13}C NMR (126 MHz, DMSO-d$_6$) δ: 165.2, 156.6, 143.5, 126.6, 114.5, 65.3, 56.3, 50.0, 35.3, 34.3, 31.9, 24.7, 16.5. LC-MS: purity 100% t_R = 5.37, (ESI) *m/z* [M + H]$^+$ 264.10. Analysis calculated for $C_{19}H_{32}NO_{5.5}$: C, 62.95; h, 8.83; N, 3.87%. Found: C, 63.10; h, 8.99; N, 3.87%.

3-(4-(tert-Butyl)phenoxy)-N,N-diethylpropan-1-amine hydrogen oxalate (**7**)

The title compound was prepared using diethylamine (0.37 g, 5 mmol) and 4-*tert*-butylphenoxy propyl bromide (1.36 g, 5 mmol). Yield 10%, m.p. 105–108 °C, $C_{17}H_{29}NO \times C_2H_2O_4 \times 1.5H_2O$ (MW = 380.49). ^{1}H NMR (300 MHz, DMSO-d$_6$) δ: 7.28 (d, *J* = 8.79 Hz, 2H), 6.84 (d, *J* = 8.79 Hz, 2H), 4.00 (t, *J* = 5.86 Hz, 2H), 3.14 (quin, *J* = 7.33 Hz, 6H), 1.95–2.13 (m, 2H), 1.04–1.34 (m, 15H). ^{13}C NMR (126 MHz, DMSO-d$_6$) δ: 164.2, 156.5, 143.5, 126.6, 114.5, 65.2, 48.4, 46.7, 34.3, 31.9, 23.7, 9.0. LC-MS: purity 100% t_R = 5.42, (ESI) *m/z* [M + H]$^+$ 264.24. Analysis calculated for $C_{19}H_{34}NO_{6.5}$: C, 59.97; h, 8.94; N, 3.68%. Found: C, 60.05; h, 8.52; N, 3.45%.

3-(4-(tert-Butyl)phenoxy)-N,N-diisopropylpropan-1-amine hydrogen chloride (**8**)

The title compound was prepared using diizopropylamine (0.51 g, 5 mmol) and 4-*tert*-butylphenoxy propyl bromide (1.36 g, 5 mmol). Yield 5%, m.p. 193–195 °C, $C_{19}H_{33}NO \times HCl$ (MW = 327.92). ^{1}H NMR (500 MHz, DMSO-d$_6$) δ: 10.01–10.36 (m, 1H), 7.26 (d, *J* = 8.59 Hz, 2H), 6.82 (d, *J* = 8.59 Hz, 2H), 3.97 (t, *J* = 6.01 Hz, 2H), 3.29–3.36 (m, 8H), 3.07–3.20 (m, 2H), 2.73 (s, 6H), 2.00–2.14 (m, 2H), 1.21 (s, 9H). ^{13}C NMR (126 MHz, DMSO-d$_6$) δ: 156.5, 143.5, 126.6, 114.5, 65.3, 54.5, 42.5, 34.3, 31.9, 24.4. LC-MS: purity 100% t_R = 5.04, (ESI) *m/z* [M + H]$^+$ 236.32.

3-(4-(tert-Butyl)phenoxy)-N,N-dipropylpropan-1-amine hydrogen oxalate (**9**)

The title compound was prepared using dipropylamine (0.51 g, 5 mmol) and 4-*tert*-butylphenoxy propyl bromide (1.36 g, 5 mmol). Yield 25%, m.p. 139–142 °C, $C_{19}H_{33}NO \times C_2H_2O_4$ (MW = 381.51). ^{1}H NMR (300 MHz, DMSO-d$_6$) δ: 7.28 (d, *J* = 8.79 Hz, 2H), 6.83 (d, *J* = 8.79 Hz, 2H), 4.00 (t, *J* = 5.86 Hz, 2H), 3.05–3.23 (m, 2H), 2.79–3.05 (m, 4H), 1.95–2.13 (m, 2H), 1.49–1.76 (m, 4H), 1.23 (s, 9H), 0.88 (t, *J* = 14.70 Hz, 6H). ^{13}C NMR (126 MHz, DMSO-d$_6$) δ: 165.1, 156.5, 143.5, 126.6, 114.5, 65.3, 54.0, 49.5, 34.3, 31.9, 23.8, 17.2, 11.5. LC-MS: purity 100% t_R = 5.89, (ESI) *m/z* [M + H]$^+$ 292.21. Analysis calculated for $C_{21}H_{35}NO_5$: C, 66.11; h, 9.25; N, 3.67%. Found: C, 65.80; h, 9.26; N, 3.60%.

1-(3-(4-(tert-Butyl)phenoxy)propyl)-2,6-dimethylpiperidine hydrogen chloride (**11**)

The title compound was prepared using 2,6-dimethylpiperidine (0.57 g, 5 mmol) and 4-*tert*-butylphenoxy propyl bromide (1.36 g, 5 mmol). Yield 10%, m.p. 194–196 dec °C,$C_{20}H_{33}NO \times HCl \times 0.25H_2O$ (MW = 344.46). ^{1}H NMR (DMSO-d$_6$, 500 MHz) δ: 9.7 (br s, 1H), 7.24 (d, *J* = 8.9 Hz, 2H), 6.79–6.85 (m, 2H), 4.00 (t, 2H, *J* = 5.4 Hz), 3.23 (br s, 4H), 1.90–2.09 (m, 2H), 1.78 (br d, 2H, *J* = 12.9 Hz), 1.39–1.66 (m, 4H), 1.20–1.29 (m, 6H), 1.19 (s, 9H). ^{13}C NMR (126 MHz, DMSO-d$_6$) δ: 156.4, 143.6, 126.7, 126.6, 114.5, 114.4, 64.9, 60.7, 58.3, 44.7, 34.3, 32.0, 31.8, 25.3, 22.5, 21.3, 18.1, 17.3. LC-MS: purity 100% t_R = 5.83, (ESI) *m/z* [M + H]$^+$ 304.37. Analysis calculated for $C_{25}H_{34.5}NO_{1.25}Cl$: C, 69.67; h, 10.02; N, 4.07%. Found: C, 69.93; h, 10.49; N, 3.94%.

1-(3-(4-(tert-Butyl)phenoxy)propyl)-2-methylpyrrolidine hydrogen oxalate (**13**)

The title compound was prepared using 2-methylpyrrolidine (0.43 g, 5 mmol) and 4-*tert*-butylphenoxy propyl bromide (1.36 g, 5 mmol). Yield 10%, m.p. 109–111 °C, $C_{18}H_{29}NO \times C_2H_2O_4$ (MW = 365.47). ^{1}H NMR (500 MHz, DMSO-d$_6$) δ: 7.25 (d, *J* = 8.59 Hz, 2H), 6.82 (d, *J* = 8.88 Hz, 2H), 3.93–4.03 (m, 2H), 3.48–3.62 (m, 1H), 3.34 (d, *J* = 7.73 Hz, 2H), 2.92–3.14 (m, 2H), 2.00–2.17 (m, 3H), 1.81–1.96 (m, 2H), 1.52–1.66 (m, 1H), 1.28 (d, *J* = 6.30 Hz, 3H), 1.20 (s, 9H). ^{13}C NMR (126 MHz, DMSO-d$_6$) δ: 165.4, 156.6, 143.4, 126.6, 114.5, 65.4, 63.2, 52.7, 49.6, 34.3, 31.9, 31.4, 25.7, 21.4, 15.7. LC-MS: purity 100% t_R = 5.46, (ESI) *m/z* [M + H]$^+$ 276.32. Analysis calculated for $C_{20}H_{31}NO_5$: C, 65.73; h, 8.55; N, 3.83%. Found: C, 65.53; h, 8.82; N, 3.71%.

4-(3-(4-(tert-Butyl)phenoxy)propyl)morpholine hydrogen oxalate (**14**)

The title compound was prepared using morpholine (0.44 g, 5 mmol) and 4-*tert*-butylphenoxy propyl bromide (1.36 g, 5 mmol). Yield 19%, m.p. 188–192 °C, $C_{17}H_{27}NO_2 \times C_2H_2O_4$ (MW = 367.44). ^{1}H NMR (300 MHz, DMSO-d$_6$) δ: 7.27 (d, *J* = 8.79 Hz, 2H), 6.83 (d, *J* = 8.79 Hz, 2H), 3.97 (t, *J* = 6.15 Hz, 2H), 3.72 (br. s., 4H), 2.92 (br. s., 6H), 1.88–2.09 (m, 2H), 1.03–1.37 (m, 9H). ^{13}C NMR (126 MHz, DMSO-d$_6$) δ: 164.6, 156.6, 143.4, 126.6, 114.5, 65.6, 64.7, 54.4, 52.2, 34.3, 31.9, 24.4. LC-MS: purity 97% t_R = 4.97, (ESI) *m/z* [M + H]$^+$ 278.19. Anal calculated for $C_{19}H_{29}NO_{6.5}$: C, 62.11; h, 7.96; N, 3.81%. Found: C, 61.96; h, 8.41; N, 3.69%.

1-(3-(4-(tert-Butyl)phenoxy)propyl)-4-methylpiperazine hydrogen oxalate (**15**)

The title compound was prepared using 4-methylpiperazine (0.50 g, 5 mmol) and 4-*tert*-butylphenoxy propyl bromide (1.36 g, 5 mmol). Yield 19%, m.p. 172 dec °C, $C_{18}H_{30}N_2O \times 2C_2H_2O_4$ (MW = 470.52). ^{1}H NMR (300 MHz, DMSO-d$_6$) δ: 7.26 (d, *J* = 8.79 Hz, 2H), 6.81 (d, *J* = 8.79 Hz, 2H), 3.95 (t, *J* = 6.15 Hz, 2H), 3.02 (br. s., 4H), 2.53–2.88 (m, 9H), 1.88 (quin, *J* = 6.45 Hz, 2H), 1.22 (s, 9H). ^{13}C NMR (126 MHz, DMSO-d$_6$) δ: 163.9, 156.8, 143.2, 126.6, 114.4, 65.8, 54.0, 52.7, 50.2, 43.2, 34.3, 31.9, 26.0. LC-MS: purity 100% t_R = 4.39, (ESI) *m/z* [M + H]$^+$ 291.22. Analysis calculated for $C_{22}H_{34}N_2O_9$: C, 56.16; h, 7.28; N, 5.95%. Found: C, 56.19; h, 7.43; N, 6.04%.

1-(3-(4-(tert-Butyl)phenoxy)propyl)-4-phenylpiperazine hydrogen oxalate (**16**)

The title compound was prepared using 4-phenylpiperazine (0.81 g, 5 mmol) and 4-*tert*-butylphenoxy propyl bromide (1.36 g, 5 mmol). Yield 15%, m.p. 164–166 °C, $C_{23}H_{32}N_2O \times C_2H_2O_4$ (MW = 442.56). ^{1}H NMR (300 MHz, DMSO-d$_6$) δ: 7.18–7.33 (m, 4H), 6.97 (d, *J* = 8.21 Hz, 2H), 6.77–6.91 (m, 3H), 4.00 (t, *J* = 5.86 Hz, 2H), 3.40 (br. s., 4H), 3.14 (br. s., 6H), 1.97–2.17 (m, 2H), 1.23 (s, 9H). ^{13}C NMR (126 MHz, DMSO-d$_6$) δ: 164.6, 156.6, 150.5, 143.4, 129.6, 126.6, 120.2, 116.3, 114.5, 65.6, 54.0, 51.8, 46.7, 34.3, 31.9, 24.7. LC-MS: purity 100% t_R = 6.01, (ESI) *m/z* [M + H]$^+$ 353.22. Analysis calculated for $C_{25}H_{34}N_2O_5$: C, 67.85; h, 7.68; N, 6.33%. Found: C, 67.77; h, 8.12; N, 6.28%.

(*Z*)*-1-(3-(4-(tert-Butyl)phenoxy)propyl)-4-(3-phenylallyl)piperazine hydrogen oxalate* (**17**)

The title compound was prepared using 1-cinnamylpiperazine (1.01 g, 5 mmol) and 4-*tert*-butylphenoxy propyl bromide (1.36 g, 5 mmol). Yield 19%, m.p. 217–219 °C, $C_{26}H_{36}N_2O \times 2C_2H_2O_4$ (MW = 572.67). ^{1}H NMR (300 MHz, DMSO-d$_6$) δ: 7.39–7.51

(m, 2H), 7.30–7.39 (m, 2H), 7.21–7.30 (m, 3H), 6.82 (d, *J* = 8.79 Hz, 2H), 6.66 (d, *J* = 15.82 Hz, 1H), 6.20–6.38 (m, 1H), 3.97 (t, *J* = 5.86 Hz, 2H), 3.44 (d, *J* = 6.45 Hz, 2H), 2.62–3.17 (m, 10H), 1.88–2.07 (m, 2H), 1.22 (s, 9H). ^{13}C NMR (126 MHz, DMSO-d$_6$) δ: 165.0, 163.7, 156.7, 143.3, 136.6, 135.3, 129.2, 128.5, 127.0, 126.6, 114.4, 65.7, 59.0, 53.9, 51.2, 50.6, 34.3, 31.9, 25.3. LC-MS: purity 100% t_R = 6.17, (ESI) *m/z* [M + H]$^+$ 393.23.

1-(4-(3-(Piperidin-1-yl)propoxy)phenyl)ethan-1-one hydrogen oxalate (**18**)

The title compound was prepared using piperidine (0.43 g, 5 mmol) and 1-(4-(3-bromopropoxy)phenyl)ethan-1-one (1.29 g, 5 mmol). Yield 13%, m.p. 157–159 °C, $C_{16}H_{23}NO_2 \times C_2H_2O_4$ (MW = 351.44). ^{1}H NMR (500 MHz, DMSO-d$_6$) δ: 7.89 (d, *J* = 8.88 Hz, 2H), 7.00 (d, *J* = 8.88 Hz, 2H), 4.09 (t, *J* = 6.01 Hz, 2H), 2.86–3.25 (m, 6H), 2.48 (s, 3H), 2.04–2.16 (m, 2H), 1.60–1.76 (m, 4H), 1.49 (br. s., 2H). ^{13}C NMR (126 MHz, DMSO-d$_6$) δ: 196.9, 165.2, 162.6, 131.0, 130.6, 114.8, 65.9, 53.8, 52.7, 27.0, 23.9, 23.2, 22.1. LC/MS: purity: 100%, t_R = 2.95, (ESI) *m/z* [M + H]$^+$ 262.18.

1-(3-(4-Isopropylphenoxy)propyl)piperidine hydrogen oxalate (**19**)

The title compound was prepared using piperidine (0.43 g, 5 mmol) and 4-izopropylphenoxy propyl bromide (1.29 g, 5 mmol). Yield 23%, m.p. 112–115 °C, $C_{17}H_{27}NO \times C_2H_2O_4$ (MW = 351.44). ^{1}H NMR (300 MHz, DMSO-d$_6$) δ: 7.13 (d, *J* = 8.79 Hz, 2H), 6.83 (d, *J* = 8.21 Hz, 2H), 3.97 (t, *J* = 5.86 Hz, 2H), 3.09 (t, *J* = 7.60 Hz, 6H), 2.81 (spt, *J* = 6.80 Hz, 1H), 1.96–2.17 (m, 2H), 1.60–1.82 (m, 4H), 1.50 (br. s., 2H), 1.14 (d, *J* = 6.45 Hz, 6H). ^{13}C NMR (126 MHz, DMSO-d$_6$) δ: 165.2, 156.9, 141.2, 127.7, 114.8, 65.5, 54.1, 52.6, 33.1, 24.7, 24.1, 23.2, 22.0. LC-MS: purity 100% t_R = 5.03, (ESI) *m/z* [M + H]$^+$ 262.24. Analysis calculated for $C_{19}H_{29}NO_5$: C, 64.93; h, 8.32; N, 3.99%. Found: C, 64.52; h, 8.49; N, 3.89%.

1-(3-(4-Ethylphenoxy)propyl)piperidine hydrogen oxalate (**20**)

The title compound was prepared using piperidine (0.43 g, 5 mmol) and 4-ethylphenoxy propyl bromide (1.22 g, 5 mmol). Yield 37%, m.p. 144–146 °C, $C_{16}H_{25}NO \times C_2H_2O_4$ (MW = 337.48). ^{1}H NMR (300 MHz, DMSO-d$_6$) δ: 7.10 (d, *J* = 8.79 Hz, 2H), 6.82 (d, *J* = 8.79 Hz, 2H), 3.97 (t, *J* = 5.86 Hz, 2H), 2.79–3.42 (m, 6H), 2.52 (s, 1H), 1.95–2.16 (m, 2H), 1.59–1.83 (m, 4H), 1.51 (br. s., 2H), 1.12 (t, *J* = 7.62 Hz, 3H). ^{13}C NMR (126 MHz, DMSO-d$_6$) δ: 165.2, 156.8, 136.5, 129.2, 114.9, 65.5, 54.1, 52.7, 27.8, 24.1, 23.2, 22.0, 16.5. LC/MS: purity: 100%, t_R = 4.52, (ESI) *m/z* [M + H]$^+$ 248.22.

1-(3-(p-Tolyloxy)propyl)piperidine hydrogen oxalate (**21**)

The title compound was prepared using piperidine (0.43 g, 5 mmol) and 4-methylphenoxy propyl bromide (1.14 g, 5 mmol). Yield 21%, m.p. 160–162 °C, $C_{15}H_{23}NO \times C_2H_2O_4$ (MW = 323.43). ^{1}H NMR (300 MHz, DMSO-d$_6$) δ: 7.07 (d, *J* = 8.21 Hz, 2H), 6.80 (d, *J* = 8.21 Hz, 2H), 3.96 (t, *J* = 5.86 Hz, 2H), 2.93–3.24 (m, 6H), 2.21 (s, 3H), 2.00–2.13 (m, 2H), 1.63–1.79 (m, 4H), 1.50 (br. s., 2H). ^{13}C NMR (126 MHz, DMSO-d$_6$) δ: 165.3, 156.7, 130.4, 129.9, 114.8, 65.5, 54.0, 52.6, 24.1, 23.1, 22.0, 20.6. LC/MS: purity: 98.9%, t_R = 3.98, (ESI) *m/z* [M + H]$^+$ 234.20.

1-(3-(4-Fluorophenoxy)propyl)piperidine hydrogen oxalate (**22**)

The title compound was prepared using piperidine (0.43 g, 5 mmol) and 4-fluorophenoxy propyl bromide (1.17 g, 5 mmol). Yield 15%, m.p. 132–136 °C, $C_{14}H_{19}NOF \times C_2H_2O_4$ (MW = 327.38). ^{1}H NMR (300 MHz, DMSO-d$_6$) δ: 7.10 (t, *J* = 8.79 Hz, 2H), 6.89–6.98 (m, 2H), 3.99 (t, *J* = 5.86 Hz, 2H), 2.89–3.25 (m, 6H), 1.98–2.16 (m, 2H), 1.62–1.80 (m, 4H), 1.50 (br. s., 2H). ^{13}C NMR (126 MHz, DMSO-d$_6$) δ: 165.3, 158.0, 156.2, 155.1, 155.1, 116.5, 116.3, 116.3, 116.2, 66.1, 54.0, 52.6, 24.0, 23.1, 22.0. LC/MS: purity: 98.7%, t_R = 3.57, (ESI) *m/z* [M + H]$^+$ 238.12.

1-(3-(4-chlorophenoxy)propyl)piperidine hydrogen oxalate (**23**)

The title compound was prepared using piperidine (0.43 g, 5 mmol) and 4-chlorophenoxy propyl bromide (1.25 g, 5 mmol). Yield 54%, m.p. 158–160 °C, $C_{14}H_{20}NOCl \times C_2H_2O_4$ (MW = 348.73). ^{1}H NMR (300 MHz, DMSO-d$_6$) δ: 7.31 (d, *J* = 8.79 Hz, 2H), 6.94 (d, *J* = 8.79 Hz, 2H), 4.00 (t, *J* = 5.86 Hz, 2H), 2.87–3.29 (m, 6H), 2.00–2.17 (m, 2H), 1.59–1.81 (m, 4H), 1.50

(br. s., 2H). ^{13}C NMR (126 MHz, DMSO-d$_6$) δ: 165.3, 157.6, 129.8, 125.0, 116.8, 65.9, 53.9, 52.6, 23.9, 23.1, 22.0. LC/MS: purity: 100%, t_R = 4.11, (ESI) *m/z* [M + H]$^+$ 254.13.

1-(3-(2-(tert-Butyl)phenoxy)propyl)piperidine hydrogen oxalate (**24**)

The title compound was prepared using piperidine (0.43 g, 5 mmol) and 2-*tert*-butylphenoxy propyl bromide (1.36 g, 5 mmol). Yield 8%, m.p. 184 dec °C, $C_{18}H_{29}NO \times C_2H_2O_4 \times 0.25H_2O$ (MW = 369.98). ^{1}H NMR (300 MHz, DMSO-d$_6$) δ: 7.11–7.27 (m, 2H), 6.93 (d, *J* = 7.62 Hz, 1H), 6.86 (t, *J* = 7.30 Hz, 1H), 4.03 (t, *J* = 6.15 Hz, 2H), 2.95–3.28 (m, 6H), 2.08–2.24 (m, 2H), 1.64–1.82 (m, 4H), 1.52 (d, *J* = 3.52 Hz, 2H), 1.32 (s, 9H). ^{13}C NMR (126 MHz, DMSO-d$_6$) δ: 165.2, 157.5, 137.6, 127.7, 126.8, 120.9, 112.9, 65.5, 54.4, 52.8, 34.9, 30.3, 24.4, 23.3, 22.1. LC-MS: purity 98.6% t_R = 5.24, (ESI) *m/z* [M + H]$^+$ 276.20. Analysis calculated for $C_{20}H_{31.5}NO_{5.25}Cl$: C, 64.87; h, 8.51; N, 3.79%. Found: C, 65.08; h, 8.49; N, 3.76%.

1-(3-(3-(tert-Butyl)phenoxy)propyl)piperidine hydrogen chloride (**25**)

The title compound was prepared using piperidine (0.43 g, 5 mmol) and 3-*tert*-butylphenoxy propyl bromide (1.36 g, 5 mmol). Yield 4%, m.p. 145–148 °C, $C_{18}H_{29}NO \times HCl \times 0.25H_2O$ (MW = 316.40). ^{1}H NMR (300 MHz, DMSO-d$_6$) δ: 10.12 (br. s., 1H), 7.20 (t, *J* = 7.91 Hz, 1H), 6.96 (d, *J* = 8.21 Hz, 1H), 6.88 (s, 1H), 6.74 (dd, *J* = 2.05, 7.91 Hz, 1H), 4.02 (t, *J* = 5.86 Hz, 2H), 3.43 (d, *J* = 11.72 Hz, 2H), 3.15 (br. s., 2H), 2.85 (br. s., 2H), 2.04–2.22 (m, 2H), 1.60–1.89 (m, 5H), 1.12–1.50 (m, 10H). ^{13}C NMR (126 MHz, DMSO-d$_6$) δ: 158.6, 152.9, 129.6, 118.3, 112.6, 111.3, 65.3, 54.0, 52.5, 35.0, 31.6, 23.9, 22.9, 21.9. LC-MS: purity 93.4% t_R = 5.39, (ESI) *m/z* [M + H]$^+$ 276.26. Analysis calculated for $C_{18}H_{30.5}NO_{1.25}Cl$: C, 68.27; h, 9.64; N, 4.45%. Found: C, 68.40; h, 9.74; N, 4.30%.

1-(3-(2-(tert-Butyl)-6-methylphenoxy)propyl)piperidine hydrogen oxalate (**26**)

The title compound was prepared using piperidine (0.43 g, 5 mmol) and 2-*tert*-butyl-6-methylphenoxy propyl bromide (1.43 g, 5 mmol). Yield 3%, m.p. 134–135 °C, $C_{19}H_{31}NO \times C_2H_2O_4$ (MW = 379.50). ^{1}H NMR (300 MHz, DMSO-d$_6$) δ: 7.11 (d, *J* = 6.45 Hz, 1H), 7.05 (d, *J* = 7.62 Hz, 1H), 6.94 (def t, 1H), 3.81 (br. s., 2H), 3.23 (br. s., 3H), 2.68–3.20 (m, 3H), 2.23 (s, 3H), 2.16 (br. s., 2H), 1.73 (br. s., 4H), 1.53 (br. s., 2H), 1.32 (s, 9H). ^{13}C NMR (126 MHz, DMSO-d$_6$) δ: 164.4, 156.5, 142.4, 131.5, 130.4, 125.3, 124.0, 69.4, 53.9, 52.7, 35.2, 31.6, 24.9, 23.2, 21.9, 17.5. LC-MS: purity 100% t_R = 5.52, (ESI) *m/z* [M + H]$^+$ 290.29.

1-(3-(2-(tert-Butyl)-5-methylphenoxy)propyl)piperidine hydrogen oxalate (**27**)

The title compound was prepared using piperidine (0.43 g, 5 mmol) and 2-*tert*-butyl-5-methylphenoxy propyl bromide (1.43 g, 5 mmol). Yield 49%, m.p. 199 dec °C, $C_{19}H_{31}NO \times C_2H_2O_4$ (MW = 379.50). ^{1}H NMR (300 MHz, DMSO-d$_6$) δ: 7.06 (d, *J* = 7.62 Hz, 1H), 6.75 (s, 1H), 6.66 (d, *J* = 7.62 Hz, 1H), 4.01 (t, *J* = 5.86 Hz, 2H), 2.78–3.29 (m, 6H), 2.07–2.29 (m, 5H), 1.71 (br. s., 4H), 1.51 (br. s., 2H), 1.14–1.39 (m, 9H). LC-MS: purity 99.3% t_R = 5.64, (ESI) *m/z* [M + H]$^+$ 290.29. Analysis calculated for $C_{21}H_{33}NO_5$: C, 66.46; h, 8.77; N, 3.69%. Found: C, 66.18; h, 8.98; N, 3.61%.

1-(3-(2-(tert-Butyl)-4-methylphenoxy)propyl)piperidine hydrogen oxalate (**28**)

The title compound was prepared using piperidine (0.43 g, 5 mmol) and 2-*tert*-butyl-4-methylphenoxy propyl bromide (1.43 g, 5 mmol). Yield 33%, m.p. 182–184 °C, $C_{19}H_{31}NO \times C_2H_2O_4$ (MW = 379.50). ^{1}H NMR (300 MHz, DMSO-d$_6$) δ: 7.00 (d, *J* = 1.76 Hz, 1H), 6.94 (d, *J* = 8.21 Hz, 1H), 6.78–6.87 (m, 1H), 3.98 (t, *J* = 6.15 Hz, 2H), 2.91–3.26 (m, 6H), 2.04–2.28 (m, 5H), 1.70 (d, *J* = 4.69 Hz, 4H), 1.51 (br. s., 2H), 1.31 (s, 9H). ^{13}C NMR (126 MHz, DMSO-d$_6$) δ: 165.1, 155.4, 137.3, 129.2, 127.7, 127.6, 112.9, 65.6, 54.4, 52.8, 34.8, 30.4, 24.5, 23.3, 22.1, 21.0. LC-MS: purity 97.7% t_R = 5.74, (ESI) *m/z* [M + H]$^+$ 290.29. Analysis calculated for $C_{21}H_{33}NO_5$: C, 66.46; h, 8.77; N, 3.69%. Found: C, 66.08; h, 9.01; N, 3.72%.

Synthesis of Compound **29**

*3-(Piperidin-1-yl)propyl (4-(tert-butyl)phenyl)carbamate hydrogen oxalate (***29***)*

To 1-(*tert*-butyl)-4-isocyanatobenzene (2.5 mmol, 0.438 g) dissolved in 20 mL of CH_3CN (HPLC purity) 3-(piperidin-1-yl)propan-1-ol [10] (2.5 mmol, 0.361 g) in 10 mL of CH_3CN

was added and refluxed for 10 h. After that time, the solution was concentrated in vacuo and purified by flash chromatography (CH_2Cl_2:CH_3OH; 80:20). The pure fractions were evaporated in vacuo and the final product was transformed into oxalic acid salt in absolute C_2H_5OH and precipitated $(C_2H_5)_2O$. The solid was crystallized from C_2H_5OH. Yield 35%, m.p. 171 dec °C, $C_{19}H_{30}N_2O_2 \times C_2H_2O_4$ (MW = 408.50). ^{1}H NMR (500 MHz, DMSO-d_6) δ: 9.54 (br. s., 1H), 7.29–7.45 (m, 2H), 7.25 (d, *J* = 8.59 Hz, 2H), 4.08 (t, *J* = 6.30 Hz, 2H), 2.82–3.33 (m, 6H), 1.88–2.11 (m, 2H), 1.68 (br. s., 4H), 1.48 (br. s., 2H), 1.20 (s, 9H). ^{13}C NMR (126 MHz, DMSO-d_6) δ: 165.1, 153.9, 145.3, 136.9, 125.9, 118.6, 62.1, 53.8, 52.6, 34.4, 31.7, 23.9, 23.1, 22.0.LC-MS: purity 100% t_R = 5.21, (ESI) *m/z* $[M + H]^+$ 319.34. Analysis calculated for $C_{21}H_3N_2O_6$: C, 61.75; h, 7.90; N, 6.86%. Found: C, 61.27; h, 8.22; N, 6.65%.

2.2. Key Reagents (Cytotoxicity and In Vivo Pharmacology Studies)

Pitolisant, 3-(4-chlorophenyl)propyl 3-piperidinopropyl ether as hydrochloride salt, was synthesized in the Department of Technology and Biotechnology of Drugs, Jagiellonian University Medical College in Kraków (Kraków, Poland).

Astrocyte medium, astrocyte growth supplement, fetal bovine serum, penicillin/streptomycin solution and poly-L-Lysine were from ScienCell Research Laboratories (Carlsbad, CA, USA).

The 3-(4,5-dimethylthazol-2-yl)-2,5-diphenyltetrazolium bromide (MTT), clorgyline (*N*-methyl-*N*-propargyl-3-(2,4-dichlorophenoxy)propylamine hydrochloride), deprenyl (*R*-(-)-deprenyl hydrochloride) and dimethyl sulfoxide were purchased from Sigma-Aldrich, Inc. (St. Louis, MO, USA).

The reagents for radioassays, i.e., β-phenylethylamine hydrochloride [ethyl-1-^{14}C], hydroxytryptamine binoxalate (serotonin binoxalate), 5-[2-^{14}C] and adenosyl-L-methionine, S-[methyl-^{14}C] were obtained from American Radiolabeled Chemicals, Inc. (St. Louis, MO, USA).

2.3. In Vitro Biological Studies

2.3.1. Histamine H_3 Receptor Affinity

Affinity to *h*H_3R stably expressed in CHO-K1 [6] or HEK293 [11] cells was evaluated in a radioligand binding assay as described previously. Briefly, 10 mM stock solutions of the test compounds in DMSO were prepared. Each compound was tested at eight concentrations ranging from 10^{-5} to 10^{-12} M (final concentration). All assays were carried out in duplicate. Crude membrane preparations were incubated with the tested compounds and [^{3}H]N^{α}-methylhistamine (radioligand; 2 nM; KD = 3.08 nM) in binding buffer (total volume 0.2 mL) for 60–90 min under continuous shaking. (R)(-)-α-methylhistamine (100 μM) [6] or pitolisant (10 μM) were used to define nonspecific binding. The radioactivity was counted in MicroBeta 2 [6] or MicroBeta Trilux [11] counter (PerkinElmer). Data were fitted to a one-site curve-fitting equation with Prism 6 (GraphPad Software, San Diego, CA, USA) and K_i values were calculated from IC_{50} values (from at least three experiments performed in duplicates) according to the Cheng−Prusoff equation [12].

2.3.2. Monoamine Oxidase B Inhibitory Activity

The precise method was described in [6]. First, compounds **4**–**32** were screened for hMAO B inhibitory activity at 1 μM concentration by the fluorometric method. *Para*-tyramine (200 μM) was used as a substrate for the enzyme and safinamide (1 μM) was used as a reference compound. IC_{50} values were evaluated for compounds that inhibited the enzyme by more than 50% of pargyline (10 μM) activity. Each experiment was performed in duplicate.

2.3.3. Modality of Monoamine Oxidase B Inhibition

Modality of hMAO B inhibition was evaluated for compounds **9** and **13** and the reference safinamide according to the method described previously [6,7]. Three concentrations of inhibitors, corresponding to their IC_{20}, IC_{50} and IC_{80} values, were used. Each experiment was performed in triplicate. K_M and V_{max} values were calculated from Michaelis–Menten

curves by nonlinear regression from the substrate. Lineweaver–Burk plots were calculated using linear regression in GraphPad Prism 6.07 (GraphPad Software, San Diego, CA, USA).

2.3.4. Reversibility of Monoamine Oxidase B Inhibition

The reversibility of the MAO inhibition was tested as described in [6,7]. Compounds **9** and **13** were tested in the concentration corresponding to their IC_{80} along with reference reversible (safinamide) and irreversible (rasagiline) MAO B inhibitors. Two variants of experiment were performed. In the first variant, enzyme and inhibitors were added to the reaction mixture at the same time with lower concentration (10 μM) of the substrate (p-tyramine). After 22 min, the concentration of the substrate was increased to 200 μM and the signal was measured for 5 h. In the second variant, inhibitors and enzyme were preincubated for 30 min before the addition of the lower concentration of the substrate, with the next steps performing analogically to the first variant.

2.3.5. Parallel Artificial Membrane Permeability

To evaluate permeability, the pre-coated PAMPA Plate System (Gentest^{TM}, Corning, Tewksbury, MA, USA) was used as we described previously [13]. Two compounds were selected for evaluation (**9** and **13**). Caffeine was used as the highly permeable reference. The concentrations of tested compounds were estimated by the LC/MS method on Waters TQ Detector Mass Spectrometer (Water Corporation, Milford, CT, USA) with the internal standard. The assay was conducted in triplicate. The permeability coefficients *Pe* (10^{-6}cm/s) were calculated using the formula provided by the manufacturer.

2.3.6. Evaluation of the Cytotoxicity of Compounds **9** and **13**

Cell Cultures

The studies were performed on a commercially-available astrocyte cell line isolated from human cerebral cortex (ScienCell Research Laboratories, San Diego, CA, USA; Cat no. 1800). The cells (passage 7–8) were seeded into a 96-well plate at an amount of 10,000 cells/well and kept in accordance with the ScienCell Research Laboratories' protocol, i.e., in astrocyte medium supplemented with 2% fetal bovine serum, 10% astrocyte growth supplement and 1% penicillin/streptomycin solution, in an atmosphere with 5% CO_2 at 37 °C. The cells were allowed to grow for 24 h and then treated with increasing concentrations of test compounds (0.01–0.25 mg/mL) for 24 and 72 h. Astrocytes in the medium on each plate (regardless of the factors tested) were used as a positive control.

All procedures were performed in a laminar chamber ensuring sterile conditions.

MTT Cell Viability Test

The viability of the astrocyte cell line was determined calorimetrically using 3-(4,5-dimethylthazol-2-yl)-2,5-diphenyltetrazolium bromide (MTT; Sigma-Aldrich Chemical Co. Ltd., Saint Louis, MO, USA) as described earlier [14]. Cells placed into 96-well plates (10,000 cells/well), after 24 h of culture in standard conditions, were exposed to compound **9**, compound **13** or pitolisant. After the incubation time (24 or 72 h) with examined drugs, 50 μL MTT solution (1 mg/mL) was added to each well of the plate for another 4 h. The method is based on the reduction of a yellow tetrazolium salt (MTT) into purple formazan crystals by mitochondrial succinate-tetrazolium reductase system which is metabolically active in viable cells [15,16]. At the end of the experiment, the cells were treated with 100 μL dimethyl sulphoxide, which enabled the release of the reaction product.

The absorbance was measured at 570 nm using a BioTek EL×800 microplate reader (BioTek, Winooski, VT, USA) and results were expressed as a percentage of the absorbance measured in control cells. The obtained values were plotted against different concentrations of each compound to calculate the viability inhibition concentration at 50% (IC_{50}) using GraphPad Prism 6.07 (GraphPad Software, Inc., San Diego, CA, USA). The experiment was repeated in quadruplicate.

For the cytotoxicity assessment in the MTT assays, each test drug was used at 8 concentrations (range: 0.01–0.25 mg/mL).

2.4. Animals and Pharmacological Treatment

The compound **13** has been examined for its in vivo activity in rats. Male Wistar rats weighing 180–240 g at the beginning of the experiments were used for the study. Animals were individually housed in standard cages with liquid and food available ad libitum, under an artificial reversed 12-h light–dark cycle with light off at 7 a.m., temperature 21–22 °C and 60–65% humidity.

Before the start of the experiments, the animals were habituated for 7 days to the conditions in the animal facility. Pharmacological treatments were carried out in the dark phase of the cycle. During the drug administration, the rats were kept in metabolic cages (Tecniplast, Italy). After an additional one day adaptation, there was a 3-day pre-treatment phase.

The compound **13** was given to intact Wistar rats to verify its impact on the metabolism of biogenic amines in the brain (cerebral amines and their metabolites concentrations as well as activities of metabolizing enzymes). Pitolisant (H_3R antagonist/inverse agonist) was employed as a reference drug [17,18]. Both drugs (3 mg/kg body mass, dissolved in 0.9% NaCl) were given subcutaneously for 6 consecutive days. Control rats were injected with 200 μL of 0.9% NaCl.

The volumes of consumed food and water, as well as urine excretion, were recorded daily and expressed in g or mL per 100 g of body mass or mL per 24 h, respectively.

The final results are given as means with SEM calculated for each 24-h period, computed from 3-day (pre-treatment phase) or 6-day (pharmacological treatment) monitoring [19,20]. All experimental procedures were undertaken according to EU directives and local ethical regulations.

2.5. Sample Preparation and Biochemical Analyzes

Rats subjected to pharmacological treatment with the compound **13** and pitolisant (reference compound) were sacrificed by decapitation 2 h after the last drug administration. Tissues were collected and properly prepared for subsequent biochemical analyzes. The brain was quickly removed from the skull and the selected structures (hypothalamus, striatum, cerebral cortex) were dissected according to the method by Glowinsky and Iversen [21], immediately frozen in liquid nitrogen and kept at −80 °C until assayed.

2.5.1. HNMT and MAOs Activities

MAO A and MAO B activities were estimated in cerebral homogenates with radioassays using 5-[2-^{14}C]-hydroxytryptamine binoxalate (final conc. 200 μM) and β-[ethyl-1-^{14}C]-phenylethylamine hydrochloride (final conc. 20 μM), as well as specific inhibitors—clorgyline and deprenyl (final conc. 10^{-9} M), respectively [22,23].

Histamine *N*-methyltransferase activity was determined radioenzymatically according to Taylor and Snyder [24] by measurements of radioactive *N*-tele-methylhistamine formed in a transmethylation reaction catalyzed by the enzyme, as previously described [25]. S-adenosyl-L-(methyl-^{14}C)-methionine was used as a donor of methyl group.

The enzyme activities are expressed as pmol/min/mg protein. Protein concentration was analyzed by Lowry's method [26].

2.5.2. HPLC Detection of Monoamines and Their Metabolites in Rat Brain Tissue Samples

The concentration of dopamine (DA), serotonin (5-HT) and noradrenaline (NA) as well as their metabolites, i.e., 3,4-dihydroxyphenylacetic acid (DOPAC), homovanillic acid (HVA), 3-methoxy-4-hydroxyphenylglycol (MHPG) and 5-hydroxyindoleacetic acid (5-HIAA) was determined in striatum (STR), hypothalamus (HPT) and cerebral cortex (CTX) with the RP-HPLC-ED method.

Cerebral samples for HPLC analysis were homogenized using an ultrasonic homogenizer (Fisher BioBlock Scientific, France) for 15 s in 150 µL homogenization solution (0.1 M $HClO_4$ containing 0.4 mM $Na_2S_2O_5$), and centrifuged at 12,000 rpm for 15 min at 4 °C. At least 100 µL of the supernatant was transferred to chromatographic tubes and kept at –80 °C until analysis. Next, 20 µL of the filtrates was injected into the HPLC system.

The Agilent 1100 chromatographic system with Waters Spherisorb ODS-1 RP C-18 chromatographic column (4.6 × 250 mm) preceded by a Zorbax SB-C18 pre-column (4.6 × 12.5 mm) was used. Column temperature was set at 35 °C and mobile phase flow at 1 mL/min. The glassy carbon working electrode was set at +0.65 V, relative to the Ag/AgCl reference electrode. The mobile phase consisted of a phosphate buffer (3.4 pH) containing: 0.15 M $NaH_2PO_4 \times H_2O$, 0.1 M Na_2EDTA, 0.5 mM Na_2OSA, 0.5 mM LiCl and addition of methanol (10%). The chromatographic data were analyzed using ChemStation, Revision-B.03.02, Agilent software [27].

The concentrations of monoamines and their metabolites in each sample were calculated from the integrated chromatographic peak area and presented in nmol/gram of wet tissue. Additionally, the ratio of metabolites to their parent amines was calculated.

2.6. Statistical Analysis

The results were expressed as means ± standard errors of the mean (SEM). All statistical analyses were performed using GraphPad Prism 6.07 program (GraphPad Software, Inc., San Diego, CA, USA).

The effect of pharmacological treatment was assessed with Paired *t*-test. For biochemical studies, statistical significance was determined by One-way ANOVA followed by post hoc Tukey's or Dunnett's multiple comparisons test.

The values $p < 0.05$ (*), $p < 0.01$ (**), and $p < 0.001$ (***) were considered significant.

3. Results and Discussion

3.1. Chemistry

Compounds **4**–**28** were synthesized as described previously [6]. First, phenoxypropyl bromides (IIa-IIl) were obtained by *O*-alkylation of a proper phenol in acetone in the presence of potassium carbonate. Such obtained compounds (IIa-IIl) were preliminarily purified and crude products were used for the reaction with proper amines as seen in Scheme 1. The final compounds were purified by flash chromatography and oily products were transformed into oxalic acid salt (except 8 and 25—hydrogen chloride). Carbamates 29–32 were synthesized from the appropriate isocyanate and 3-(piperidin-1-yl)propan-1-ol as reported by Łażewska et al. [10] (Scheme 2). The final compounds were purified by column chromatography and oily products were transformed into oxalic acid salt. The structures and purity of compounds were confirmed by ^{1}H NMR, ^{13}C NMR and LC-MS analysis (see Supplementary Materials S2).

3.2. In Vitro Pharmacological Studies

3.2.1. Histamine H_3 Receptor Affinity of Tested Compounds

Affinity for hH_3R was evaluated in a radioligand binding assay using [^{3}H]N^{α}-methyl histamine as radioligand in CHO K1 or HEK293 cells stably expressing hH_3R as described previously [6,7]. Results are presented in Tables 1–4. For comparison, DL76 (our lead structure) was tested in both assays. Results obtained for DL76 in CHO K1 cells are slightly lower (K_i = 58 nM) than in HEK293 cells (K_i = 38 nM), the same as our results for pitolisant (CHO K1 cells: K_i = 30 nM compared with published data for HEK293 cells: K_i = 12 nM [28]). At the beginning, compounds **4**–**9**, **11**, **13**–**17** and **24**–**32** were screened for the inhibition of [^{3}H]N^{α}-methylhistamine binding to the hH_3R (in CHO K1 cells) at the 1 µM concentration. Then, those with at least 50% inhibition for hH_3R were selected for further testing (K_i evaluation). In the first series (compounds **4**–**17**; Table 1), an influence of an amine moiety for hH_3R affinity was investigated. Among the acyclic amines, no correlation was observed between the length of the carbon chain (methyl to propyl; compounds **4**,**5**,**7** and **9**), or

the branching (compounds **6** or **8**) for hH_3R. The most potent was compound **9** with a K_i of 323 nM. In the cyclic amines series (compounds **10**–**17**) the highest hH_3R affinity was shown by the 2-methylpyrrolidine derivative (compound **13**) with a K_i of 25 nM. A methyl substituent at the amine ring seems profitable for hH_3R affinity. Compounds **10** (2-methyl) and **11** (2,6-dimethyl), derivatives of a piperidine with the methyl substituent, had very good affinity for hH_3R (K_i < 100 nM). Other amines (morpholine, substituted piperazines) showed no activity at all (compounds **15**, **17**) or exhibited weak potency (compounds **14**, **16**). In the second series (compounds **18**–**23**), we investigated the change of the 4-*tert*-butyl substituent at the phenyl ring for other groups: acetyl, alkyl (methyl, ethyl, isopropyl) or halogen (-Cl, -F). Compounds were tested in the binding assay in HEK293 cells [7]. All compounds showed good hH_3R affinity with K_i values below 100 nM. The change for an acetyl group (compound **18**) was the most profitable. compound **18** (K_i = 15 nM) was twice as active as DL76 (K_i = 38 nM). Next, we performed a modification of DL76 by systematically removing methyl groups from the 4-*tert*-butyl substituent of DL76 to an isopropyl (compound **19**), an ethyl (compound **20**), and a methyl (compound **21**) (Table 2). While compounds **19** and **20** exhibited slightly lower activity (K_i of 52 nM and 62 nM, respectively) than the parent DL76, compound **21** showed comparable affinity (K_i of 43 nM). Interestingly, the introduction of halogen atoms (compounds **22**, **23**) resulted in decreased hH_3R affinity (K_i > 80 nM). Further exploration of the influence of 4-*tert*-butyl position on the phenyl ring (third series: compounds **24**–**28**; Table 3) showed that the presence of a substituent at the 4 position is very important for hH_3R affinity. Compounds **24** and **25** had much lower affinity than DL76, and the 2 position was the least favorable (compound **24** with a K_i > 1000 nM). In the next step, due to the good commercial accessibility of phenols, compound **24** was subsequently modified by adding a methyl substituent at the phenyl ring to obtain compounds **26**–**28**. compound **28** with the methyl group at the 4 position had moderate affinity for hH_3R (K_i = 448 nM) whereas compounds with 5-methyl (**27**) and 6-methyl (**26**) were inactive (K_i > 1000 nM). Introduction of this second substituent led to an increase in potency compared to compound **24** with only 2-*tert*-butyl substituent at the phenyl ring. In the last series (compounds **29**–**32**; Table 4), the ether linker in DL76 was exchanged for a carbamate group (compound **29**). This probe led to a considerable decrease in hH_3R affinity for compound **29** (K_i > 1000 nM). Next, we also changed 4-*tert*-butylphenyl moiety for aliphatic substituents with the *tert*-butyl group (compounds **30**–**32**). The resulting derivatives (**30**–**32**) exhibited no affinity for hH_3R (K_i > 1000 nM). To sum up, of all investigated changes, only the replacement of the piperidine (in DL76) by a 2-methylpyrrolidine and the 4-*tert*-butyl substituent by a 4-acetyl resulted in compounds with high affinity for hH_3R.

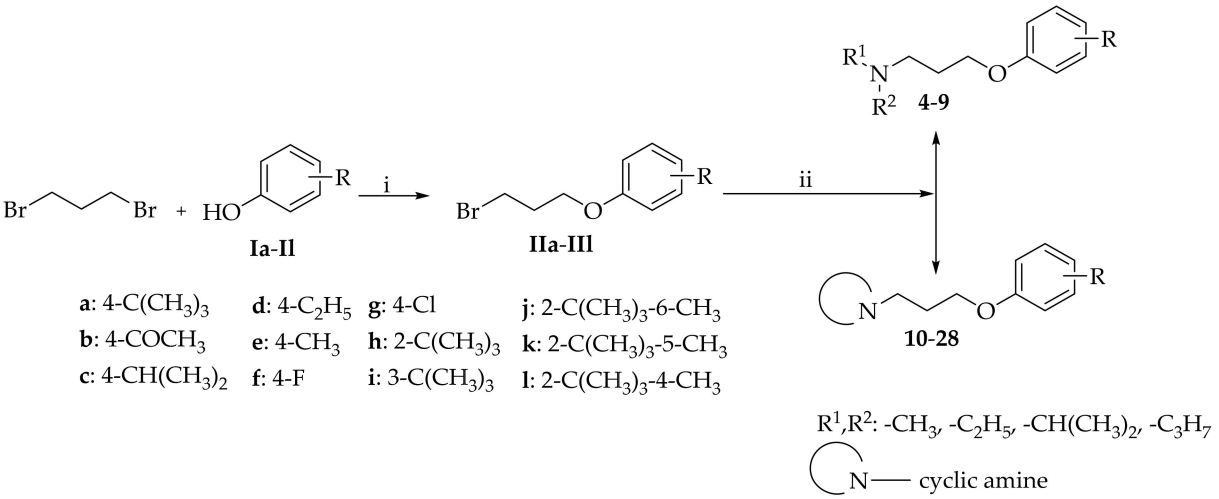

Scheme 1. The synthetic route of compounds **4**–**28**. (i) K_2CO_3, acetone, reflux 7–24 h. (ii) amine, K_2CO_3, KI, CH_3CN, reflux 24–72 h.

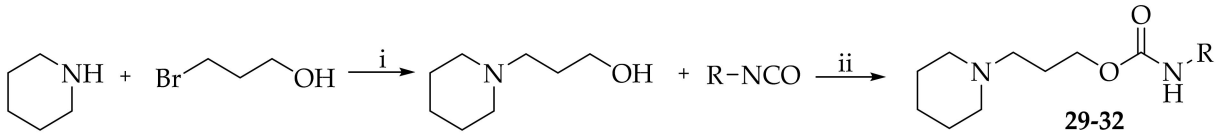

R: 4-*tert*-butylphenyl; *tert*-butyl; 2,4,4-trimethylpentane; 3,3-dimethylbutane

Scheme 2. The synthetic route of compounds **29**–**32**. (i) K_2CO_3, KI, CH_3CN, reflux 48 h (ii) CH_3CN, reflux 5–10 h.

Table 2. In vitro affinities for human histamine H_3 receptor and human MAO B inhibitory activities of the target compounds **18**–**23**.

Compound	Structure	hH_3R [a] K_i [nM] [95%CI]	hMAO B [b] IC_{50} [nM] (% of Inh.) [c]
	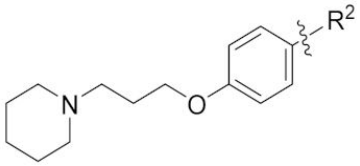		
	R^2		
18		15 [5; 45]	(19%)
19		52 [24; 113]	21 ± 3
20	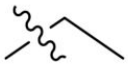	61 [21; 178]	70 ± 2
21		43 [10; 178]	755 ± 106
22		93 [16; 536]	(29%)
23		83 [12; 561]	1058 ± 37

[a]: [^{3}H]N^{α}-Methylhistamine-binding assay in HEK293 cells stably expressing the hH_3R; mean value within the 95% confidence interval (CI) of three independent experiments. [b]: fluorometric MAO assay; mean value ± SEM of 2–4 independent experiments. [c]: % of inhibition at 1 μM; mean values of two independent experiments.

3.2.2. Human MAO B Inhibitory Activity of Tested Compounds

All compounds were first screened for hMAO B inhibitory activity at the concentration of 1 μM. Then, those which showed inhibition higher than 50% were selected for further IC_{50} evaluation. The obtained results showed different abilities of tested compounds to inhibit hMAO B activity (Tables 1–4). The most potent hMAO B inhibitors were found among compounds from the first series (Table 1). All aliphatic amine derivatives (compounds **4**–**9**) exhibited IC_{50} values in low nanomolar concentration ranges (IC_{50} < 40 nM) and a dipropyl amine derivative **9** was the most potent among them (IC_{50} of 2 nM). Moreover, among cyclic amine derivatives, very potent hMAO B inhibitors were found, with IC_{50} values ≤11 nM (compounds **10**–**13**, e.g., compound **13** with an IC_{50} of 4 nM). In the other series (compounds **18**–**32**; Tables 2–4), generally, all introduced changes led to inactive or

only weak active compounds (with the exceptions of **19**: IC_{50} = 21 nM and **20**: IC_{50} = 70 nM). Based on the results, we selected compounds **9** and **13** for further analysis.

Table 3. In vitro affinities for human histamine H_3 receptor and human MAO B inhibitory activities of the target compounds **24**–**28**.

Compound	Structure	*h*H_3R [a] K_i [nM] ± SEM (% Inh.) [b]	hMAO B [c] IC_{50} [nM] (% of Inh.) [d]
	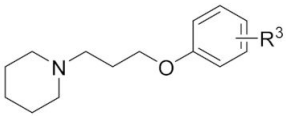		
	R^3		
24	2-*tert*-Butyl	(13%)	(4%)
25	3-*tert*-Butyl	340 ± 23	1021 ± 69
26	2-*tert*-Butyl-6-methyl	(0%)	(0%)
27	2-*tert*-Butyl-5-methyl	(0%)	(4%)
28	2-*tert*-Butyl-4-methyl	448 ± 59	(7%)

[a]: [^{3}H]N^{α}-Methylhistamine-binding assay in CHO-K1 cells stably expressing the *h*H_3R; mean value ± SEM of three independent experiments. [b]: % of radioligand inhibition at *h*H_3R (in CHO K1 cells) at 1 μM in two independent experiments, each as triplate; mean value. [c]: fluorometric MAO assay; mean value ± SEM of 2–4 independent experiments. [d]: % of inhibition at 1 μM; mean values of two independent experiments.

Table 4. In vitro affinities for human histamine H_3 receptor and human MAO B inhibitory activities of the target compounds **29**–**32**.

Compound	Structure	*h*H_3R [a] (% Inh.) [b]	hMAO B [c] IC_{50} ± SEM [nM] (% of Inh.) [d]
	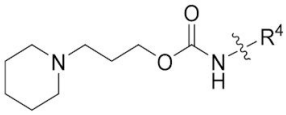		
	R^4		
29	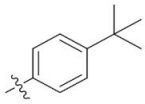	(32%)	2325 ± 436
30		(15%)	(47%)
31	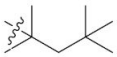	(19%)	(41%)
32	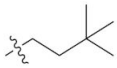	(20%)	925 ± 29

[a]: [^{3}H]N^{α}-Methylhistamine-binding assay in CHO-K1 cells stably expressing the *h*H_3R; mean value ± SEM of three independent experiments. [b]: % of radioligand inhibition at *h*H_3R (in CHO K1 cells) at 1 μM in two independent experiments, each as triplate; mean value. [c]: fluorometric MAO assay; mean value ± SEM of 2–4 independent experiments. [d]: % of inhibition at 1 μM; mean values of two independent experiments.

3.2.3. Modality of Human MAO B Reversible Inhibition of Compounds **9** and **13**

For testing modality of enzyme inhibition, we used three concentrations of inhibitors that corresponded to their IC_{20}, IC_{50} and IC_{80} values. Substrate (p-tyramine) was used at concentrations: 0.05, 0.1, 0.5, 1.0, 1.5 and 2.0 mM. For compounds **9** and **13**, K_M and V_{max} values calculated from Michaelis–Menten curves showed behavior typical for noncompetitive inhibition (V_{max} decreased curvilinearly along with the increase in inhibitor concentration, and K_M was not affected) (Table 5). On the Lineweaver–Burk double-reciprocal plot, lines

representing solvent and different concentrations of the inhibitor intersect to the left side of the y-axis and on the x-axis, suggesting a pure noncompetitive behavior. Inhibitors show noncompetitive modality when having equal affinity for both free enzyme and enzyme-substrate complex [29] (Figures 3 and 4). In the same assay conditions, safinamide showed behavior characteristic for mixed inhibition: V_{max} decreased curvilinearly and K_M increased curvilinearly with the increase in the inhibitor concentration, and lines on the Lineweaver–Burk plot intersect to the left of the y-axis and above the x-axis (Table 5). This behavior suggested that the inhibitor can bind to both free enzyme and enzyme-substrate complex but with higher affinity to the free enzyme [29].

Table 5. Effects of inhibition modalities on steady state kinetic parameters and diagnostic signatures on double-reciprocal Lineweaver–Burk plot of safinamide, **9** and **13**.

Parameter	Compound		
	Safinamide	**9**	**13**
app. K_M	↑ curvilinearly with ↑ [I]	No effect [a]	No effect [a]
app. V_{max}	↓ curvilinearly with ↑ [I]	↓ curvilinearly with ↑ [I]	↓ curvilinearly with ↑ [I]
app. V_{max}/app. K_M	↓ curvilinearly with ↑ [I]	↓ curvilinearly with ↑ [I]	↓ curvilinearly with ↑ [I]
Lines on LB plot	Lines intersect to the left of y-axis and above x-axis	Lines intersect to the left of y-axis directly on x-axis	Lines intersect to the left of y-axis directly on x-axis
Mode of inhibition from kinetic values and LB plot	Mixed mode	Noncompetitive	Noncompetitive
Affinity	Free enzyme > enzyme-substrate complex	Free enzyme ≈ enzyme-substrate complex	Free enzyme ≈ enzyme-substrate complex

[a]—no statistical difference, one-way ANOVA, ↑—increase, ↓—decrease, [I]—concentration of the inhibitor, K_M—Michaelis constant, V_{max}—maximum velocity obtained at infinite substrate concentration, app. K_M—apparent K_M, app. V_{max}—apparent V_{max}, LB—Lineweaver–Burk double-reciprocal plot.

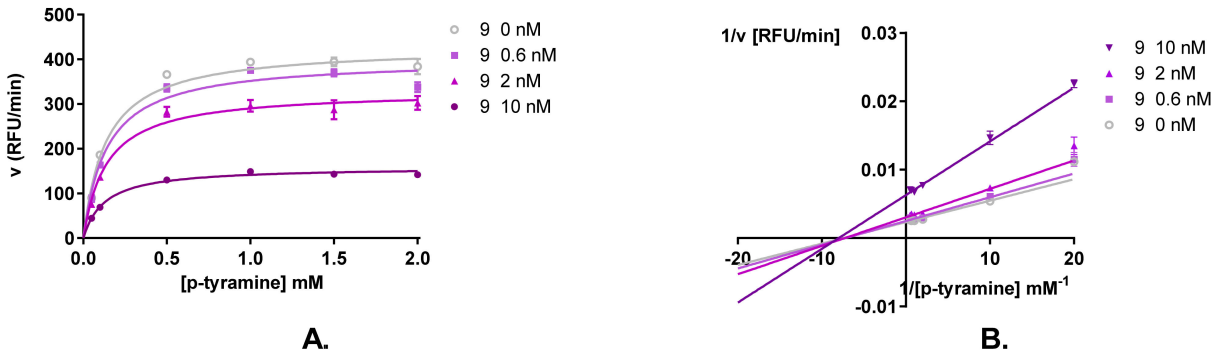

Figure 3. Michaelis–Menten curves (**A**) and Lineweaver–Burk plot (**B**) for **9**. Compound showed noncompetitive inhibition with equal affinity to the free enzyme and enzyme-substrate complex.

For MAO B inhibition and using p-tyramine as substrate, compounds **9** and **13** showed more promising behavior than safinamide. In the human body where substrates for MAO B are present and their concentration changes, the equal affinity to free enzyme and enzyme-substrate complex could prove to be an asset.

3.2.4. Reversibility of Monoamine Oxidase B Inhibition of Compounds **9** and **13**

Curves on the Figure 5A,B represent the reactivation of the MAO B activity after the addition of the excess amount of the substrate (p-tyramine 200 uM) to the enzyme that had been firstly inhibited by reference and tested compounds in concentrations corresponding to their IC_{80}. Irreversible inhibition by rasagiline was clearly shown as the line that represents

the amount of the product of the MAO B remained flat even after the addition of the excess amount of the substrate. In contrast, for the lines that represent safinamide, **9** and **13** showed an increase in the product amount with increase in substrate concentration which suggested reversible inhibition. Additionally, comparing the curves for two variants of the reversibility testing with and without preincubation (Figure 5C,D), safinamide and compounds **9** and **13** did not show differences between the variants which suggested very quick inhibition (i.e., noncovalent bonding), while preincubated rasagiline inhibited the enzyme more strongly than non-preincubated (as irreversible and mechanism-based inhibitor rasagiline requires time to be metabolised by MAO B to its reactive form which then forms covalent bonds with the enzyme [30]).

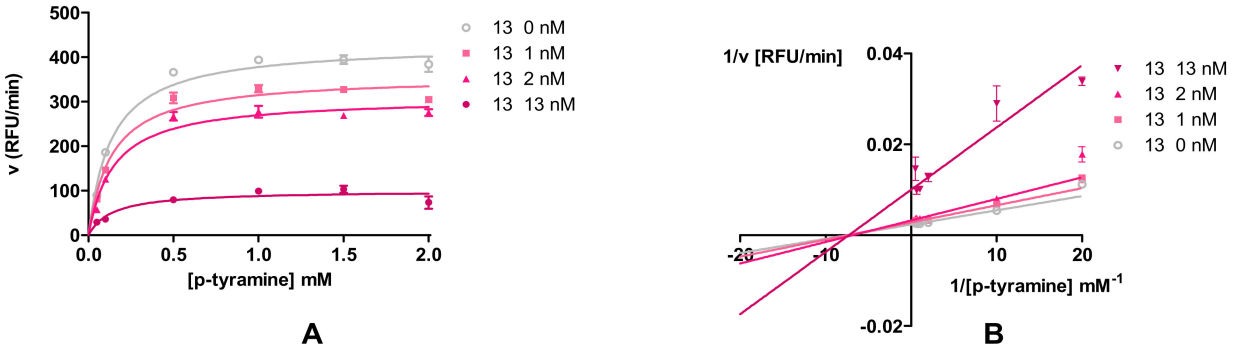

Figure 4. Michaelis–Menten curves (**A**) and Lineweaver–Burk (**B**) plot for **13**. Compound showed noncompetitive inhibition with equal affinity to the free enzyme and enzyme-substrate complex.

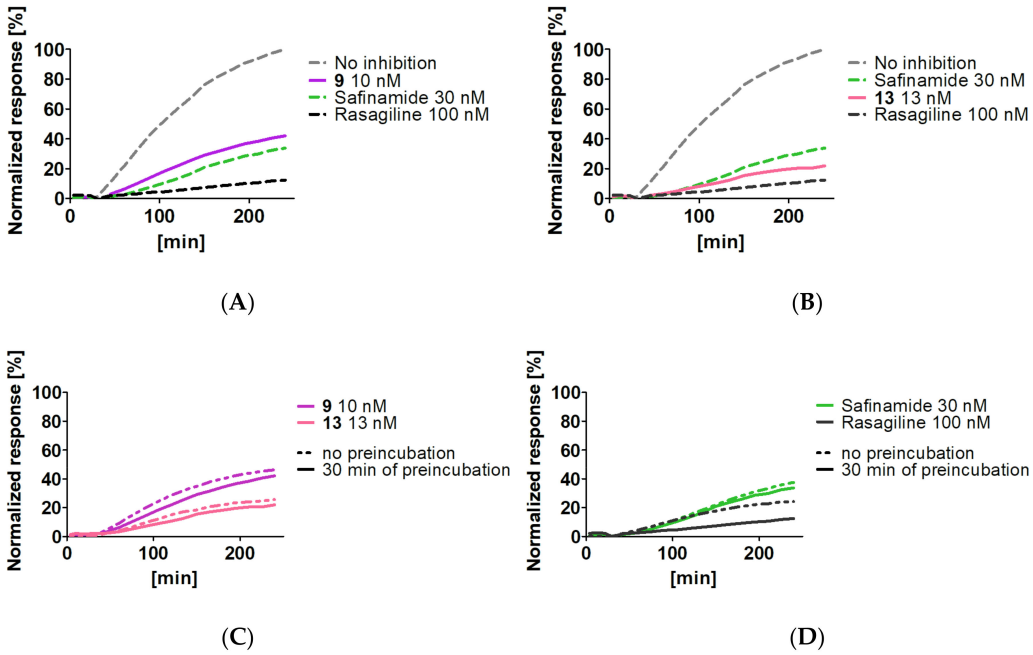

Figure 5. Reactivation of MAO activity after addition of excess amount of substrate (p-tyramine 200 μM) to the enzyme previously inhibited by irreversible (rasagiline), reversible (safinamide) and tested inhibitors in concentrations corresponding to their IC_{80}. Only the variant with preincubation was shown on the chart to not disturb the readability (**A**,**B**). Comparison of curves from preincubated and non-preincubated variant of experiment: preincubated rasagiline inhibited the enzyme more strongly than non-preincubated, while safinamide, **9** and **13** showed almost no differences between preincubated and non-preincubated samples (**C**,**D**).

3.2.5. Permeability of Compounds **9** and **13**

For compounds acting on the CNS, the ability to cross the blood–brain barrier (BBB) is very important. It is good to assess this property before starting in vivo studies. Therefore, the permeability of the two most potent hMAO B inhibitors (compound **9** and **13**) was assessed using the Parallel Artificial Membrane Permeability Assay (PAMPA). This commercially available method assesses the passive transport of compounds. The assay is performed in multiwell microplates, which consist of an acceptor part and a donor part, separated by a lipid-saturated microporous filter. The results of the test are summarized in Table 6. Only for the compound **13** was it possible to calculate the permeability coefficient (P_e). The results showed that the compound **9** was not able to cross the artificial membrane, as no mass peak of the compound was observed in the acceptor part. In contrast, the compound **13** had a high permeability, as the calculated P_e (P_e = 16.72 × 10^{-6} cm/s) was very high and comparable to caffeine (P_e = 15.1 × 10^{-6} cm/s).

Table 6. Permeability coefficient of compounds **9** and **13** and caffeine.

Compound	[a,b] P_e (×10^{-6}cm/s) ± SD
9	—— [c]
13	16.72 ± 0.06
caffeine	15.1 ± 0.4

[a]: PAMPA plate's manufacturer breakpoint for permeable compounds: $P_e \geq 1.5 \times 10^{-6}$ cm/s. [b]: tested in triplicate. [c]: the compound has not passed; no peak in the acceptor part.

3.2.6. Effect of Compounds **9** and **13** on the Viability of Human Astrocyte Cell Lines

In the next step, we investigated the effect of two of the most promising hybrids, compounds **9** and **13**, on the viability of human astrocyte cell lines after 24 h and 72 h of incubation. Pitolisant, the known H_3R ligand, was used as a reference drug [17]. The examined compounds were applied in 8 concentrations (from 0.01 mg/mL to 0.25 mg/mL). Their effects on the viability of astrocytes after 24 h of incubation are presented in Figure 6. According to the obtained data, the two lowest concentrations of tested compounds (i.e., 0.01 and 0.025 mg/mL) did not affect cell viability. Regarding the successive doses of the agents used, a dose-dependent decrease in cell survival was observed, which was statistically significant. The highest decline in cell viability, over 95% in comparison to the control level, was observed for compounds **9** and **13** at the concentration of 0.15 and 0.25 mg/mL.

Interestingly, the threefold extension of the incubation time with the tested compounds in the same concentration range resulted in only a slight increase in cytotoxicity. Human astrocytes after 72 h of incubation with compound **9** and **13** as well as pitolisant were characterized by a similar survival rate to that during exposure to the test agents for 24 h (Table 7). In general, MTT conversion tests performed on human astrocyte cell lines showed slightly higher toxicity of compound **9** and **13** compared to pitolisant, which is documented by the calculated IC_{50} values (Table 7), with higher values indicating lower cytotoxicity reported for compound **13**.

Table 7. IC_{50} values obtained for compounds **9** and **13** against human astrocyte cell lines assessed by MTT test.

	Compound 9	Compound 13	Pitolisant
IC_{50} 24 h	144.16 µM (0.055 mg/mL)	229.84 µM (0.084 mg/mL)	346.06 µM (0.115 mg/mL)
IC_{50} 72 h	123.19 µM (0.047 mg/mL)	142.28 µM (0.052 mg/mL)	240.74 µM (0.08 mg/mL)

IC_{50} values were determined after 24 h and 72 h of incubation of human astrocytes with compound **9,** compound **13** or pitolisant at doses: 0.01–0.25 mg/mL (6 experiments).

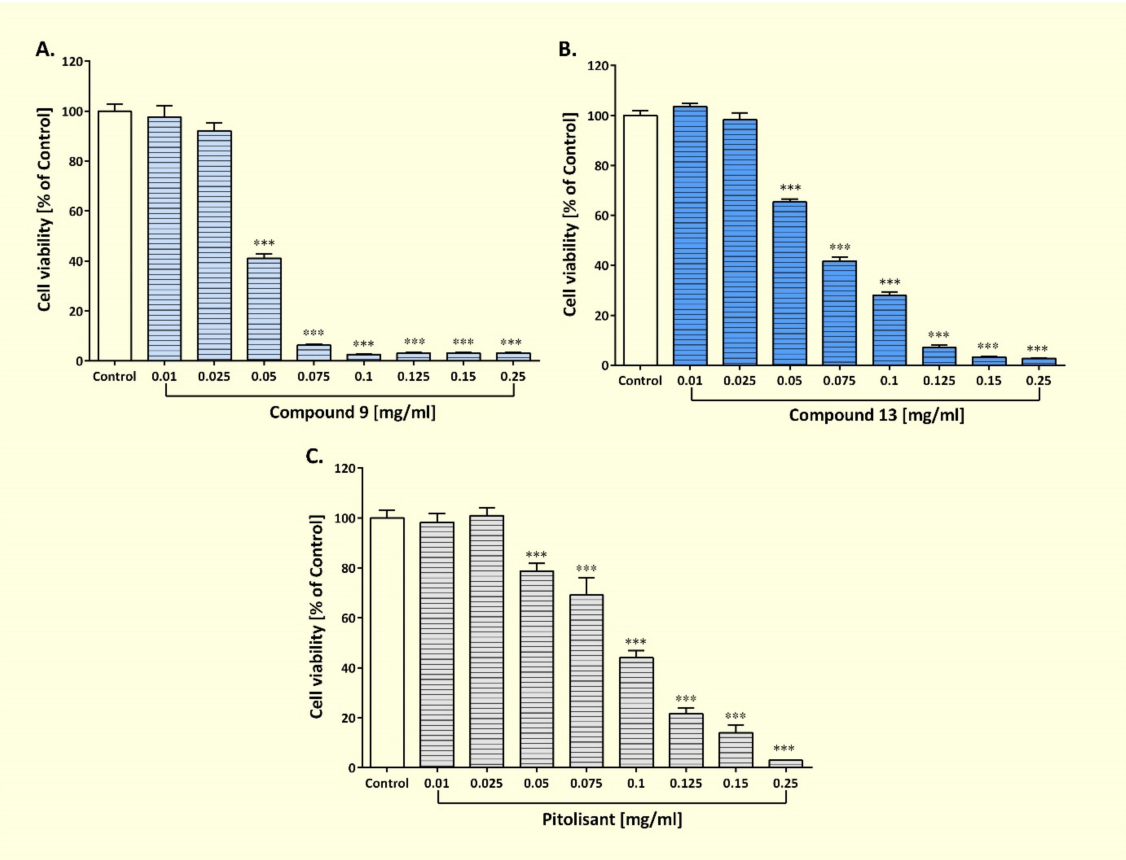

Figure 6. The effects of compound **9** (**A**), **13** (**B**) and pitolisant (**C**) on the viability of human astrocytes after 24 h of incubation. Bars represent the means ± SEM of 6 experiments and expressed as percentage of untreated control cells. One-way ANOVA and Dunnett's multiple comparisons test: *** $p < 0.001$ vs. corresponding control (untreated cells).

3.3. Preliminary Verification of In Vivo Activity of the Compound **13**

The presented research focused on the search for new multifunctional compounds combining the properties of an MAO B inhibitor and the H_3R. Taking into account the results of in vitro studies on the affinity for hH_3R and hMAO B inhibitory activity (hH_3R: K_i = 25 nM; hMAO B: IC_{50} = 4 nM; Table 1) as well as low cytotoxicity (Table 7), and predicted very good in vivo permeability in the PAMPA assay (Table 6), the compound **13** was selected for in vivo studies. Thus, if H_3R antagonists cross the BBB, they should affect food intake [18,31]. Experiments were conducted as described previously [20,32,33].

The assessment concerned the effects of compound **13** on the feeding behavior of rats after its repeated peripheral injections, and the influence on metabolism and concentration of selected key neurotransmitters. Pitolisant was used as the reference drug in in vivo studies [17].

3.3.1. Effect on Sub-Chronic Administration of compound **13** on Feeding Behavior

The effect of sub-chronic administration of compound **13** and pitolisant on food and water consumption as well as urine output is presented in Figure 7.

In the compound **13**-treated group, a statistically significant decline in food consumption was noted, compared with the results obtained before the drug's administration (8.61 ± 0.11 vs. 10.63 ± 0.37 g/100 g bw; paired *t*-test, $p < 0.001$). compound **13** affected the feeding pattern more than pitolisant (8.95 ± 0.14 vs. 10.57 ± 0.42 g/100 g bw; paired *t*-test, $p < 0.01$). In addition, rats injected with compound **13** had lower water consumption, expressed in mL/100 g bw/24 h (13.37 ± 0.31 vs. 15.035 ± 0.37; paired *t*-test, $p < 0.05$) and decreased urine output (8.90 ± 0.045 vs. 10.08 ± 0.35 mL/24 h; paired *t*-test, $p < 0.01$), compared to the pre-treatment period.

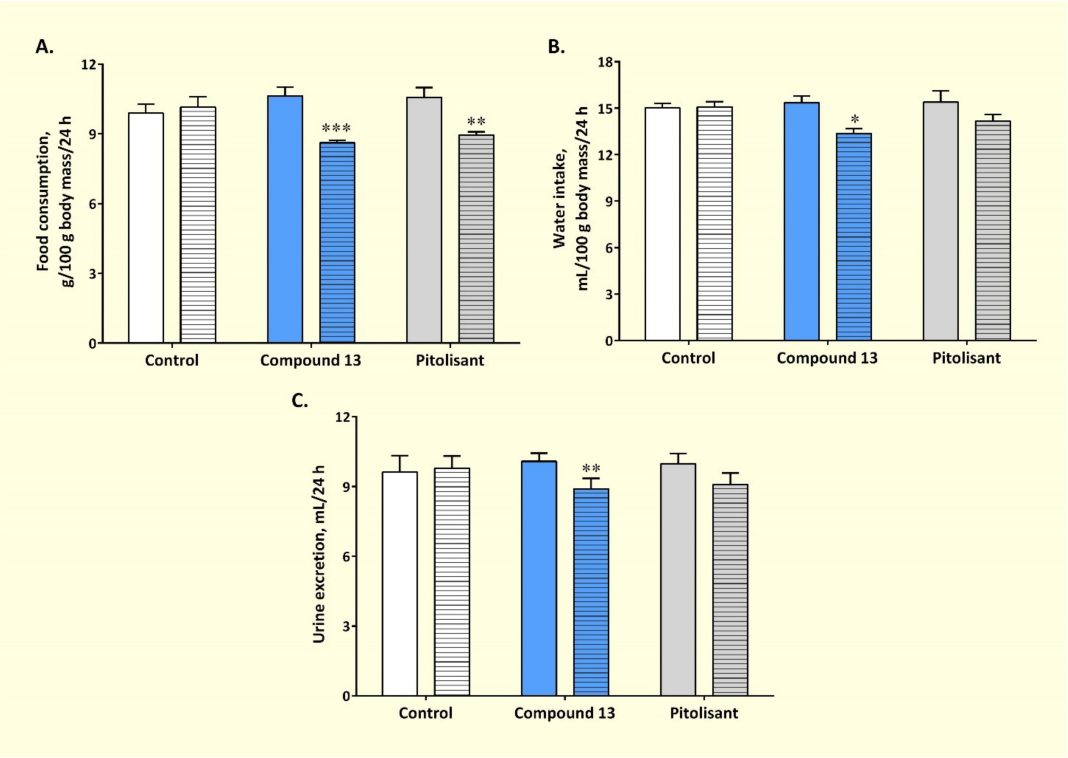

Figure 7. The effect of sub-chronic administration of the compound **13** on food (**A**) and water (**B**) consumption, and urine output (**C**). Pitolisant, a histamine H_3 receptor antagonist/inverse agonist, was employed as the reference compound. The tested compounds (both in a dose of 3 mg/kg of body mass) were injected subcutaneously for 6 consecutive days. The values are mean ± SEM. The bars without a pattern correspond to the 3-day pre-test monitoring, whereas bars with pattern correspond to the 6-day treatment period with appropriate drugs. Paired *t*-test: * $p < 0.05$, ** $p < 0.01$ or *** $p < 0.001$ vs. pre-test (i.e., before treatment).

Subcutaneous administration of pitolisant to rats for 6 days also resulted in reduced water consumption and urine excretion, although these changes were not statistically significant (14.16 ± 0.43 vs. 15.39 ± 0.43 mL/100 g bw/24 h and 9.08 ± 0.49 vs. 9.98 ± 0.44 mL/24 h, respectively).

In the control group, which was administered 0.2 mL of physiological saline, no changes in the consumption of feed and water nor in urine excretion were observed in both tested time intervals.

3.3.2. Activity of MAOs and HNMT in Rat Cerebral Cortex after Sub-Chronic Administration of Compound **13**

In the concentration used, compound **13** caused more than 90% decline in MAO B activity in rat cerebral cortex (Figure 8), whereas MAO A activity was inhibited only by 12% (data not shown).

The activity of MAO B was significantly reduced after administration of compound **13** at a dose of 3 mg/kg/day for 6 days, compared to the control group (48.38 ± 12.02 vs. 584.50 ± 19.14 pmol/min/mg protein; one-way ANOVA and Tukey's multiple comparisons test, $p < 0.001$). In the pitolisant-treated group, MAO A and B activities were close to that recorded in control animals.

Compound **13** did not influence HNMT activity. Similar activity of HNMT was noted in all studied groups, i.e., in the compound **13** group—40.09 ± 1.77, in the pitolisant group—42.51 ± 1.40, and in the control group—37.53 ± 1.22 pmol/min/mg of protein.

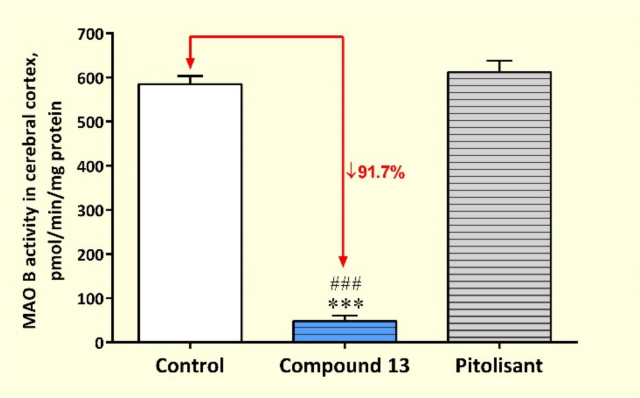

Figure 8. Effects of sub-chronic administration of compound **13** and pitolisant on rat brain MAO B activity. Values are means ± SEM for 8 rats. One-way ANOVA and Tukey's multiple comparisons test: *** vs. control, ### vs. pitolisant, $p < 0.001$.

3.3.3. Effects of Sub-Chronic Administration of Compound **13** on Cerebral Concentration of Monoamines and Their Metabolites

In the compound **13** group, a statistically significant increase in DA content in CTX and STR was noted, compared with the results obtained for control animals (CTX: 1.777 ± 0.128 vs. 1.125 ± 0.145 nmol/g wet tissue, STR: 9.914 ± 1.718 vs. 5.244 ± 0.617 nmol/g wet tissue; Figure 9A,C, left panel). In contrast to these results, six-day subcutaneous administration of compound **13** caused a decrease in DOPAC levels in CTX and STR (CTX: 0.562 ± 0.093 vs. 0.857 ± 0.029 nmol/g wet tissue, STR: 1.704 ± 0.187 vs. 2.934 ± 0.296 nmol/g wet tissue; Figure 9A,C, right panel). The concentration of DA and DOPAC in these brain structures correspond with a decline in DOPAC/DA ratio. Moreover, a decrease in the HVA/DA ratio in CTX was noted (Table 8).

Table 8. Ratio [a] of monoamines and their metabolites in different brain areas in rats—the effect of sub-chronic treatment with compound **13** and pitolisant.

Brain Region	Group	MHPG/NA	DOPAC/DA	HVA/DA	5-HIAA/5-HT
CTX	Control	1.466 ± 0.131	0.886 ± 0.107	0.391 ± 0.042	1.229 ± 0.185
	compound **13**	0.790 ± 0.275 *	0.364 ± 0.080 **,##	0.254 ± 0.015 *,##	1.211 ± 0.202
	Pitolisant	1.344 ± 0.118	0.923 ± 0.132	0.449 ± 0.035	1.105 ± 0.087
HPT	Control	0.268 ± 0.018	0.563 ± 0.075	0.328 ± 0.118	0.820 ± 0.139
	compound **13**	0.205 ± 0.030	0.359 ± 0.117	0.329 ± 0.091	0.810 ± 0.061
	Pitolisant	0.257 ± 0.021	0.538 ± 0.037	0.276 ± 0.030	0.981 ± 0.051
STR	Control	0.470 ± 0.032	0.513± 0.036	0.472 ± 0.384	3.029 ± 0.672
	compound **13**	0.329 ± 0.057	0.207 ± 0.067 *	0.486 ± 0.388	2.456 ± 0.908
	Pitolisant	0.455 ± 0.046	0.376 ± 0.074	ND	2.879 ± 0.222

[a]: The ratios of metabolites to their parent amines were calculated by dividing the metabolite concentrations by the amine concentrations (expressed in nmoles per g of wet tissue). CTX, cerebral cortex; HPT, hypothalamus; STR, striatum; NA, noradrenaline; MHPG, 3-Methoxy-4-hydroxyphenylglycol; DA, dopamine; DOPAC, 3,4-dihydroxyindoleacetic acid; HVA, homovanillic acid; 5-HT, serotonin; 5-HIAA, 5-hydroxyindole-3-acetic acid; ND, not determined. Values are means ± SEM (n = 7–8). One-way ANOVA and Tukey's multiple comparisons test: * vs. control,# vs. pitolisant. One symbol means $p < 0.05$, while two symbols $p < 0.01$.

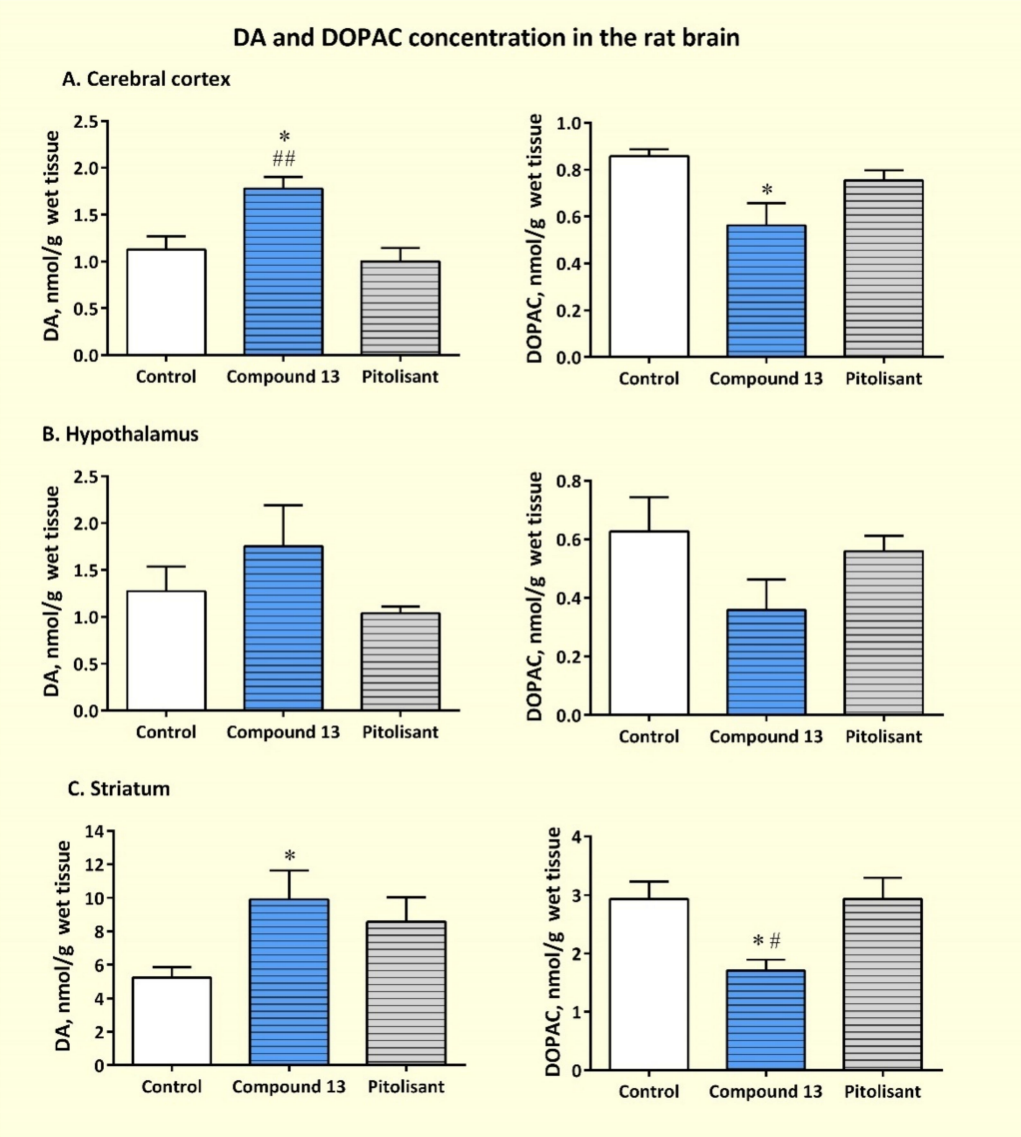

Figure 9. Concentrations of DA and DOPAC in brain regions of rats sub-chronically treated with compound **13** and pitolisant (DA—dopamine, DOPAC—3,4-dihydroxyindoleacetic acid). The drugs (both in a dose of 3 mg/kg of body mass) were injected subcutaneously for 6 consecutive days. Values are expressed as nanomoles per gram wet weight and are means ± SEM (n = 7–8). One-way ANOVA and Tukey's multiple comparisons test: * vs. control, # vs. pitolisant. One symbol means $p < 0.05$, while two symbols $p < 0.01$.

In the case of the hypothalamus, a slight increase in DA concentration and a decrease in DOPAC concentration were noted in the compound **13** group, although these changes were not statistically significant (Figure 9B).

Additionally, injections of compound **13** also slightly increased NA concentration in CTX (from 1.166 ± 0.084 to 1.255 ± 0.152 nmol/g wet tissue) and significantly decreased MHPG concentration (from 1.659 ± 0.048 to 0.897 ± 0.280 nmol/g wet tissue), expressed as a lower MHPG/NA ratio (0.79 ± 0.28 vs. 1.47 ± 0.13). These results are presented in Figure 10A and Table 8, respectively. In the other examined brain structures, no differences were found in the concentration of NA and MHPG (Figure 10B,C).

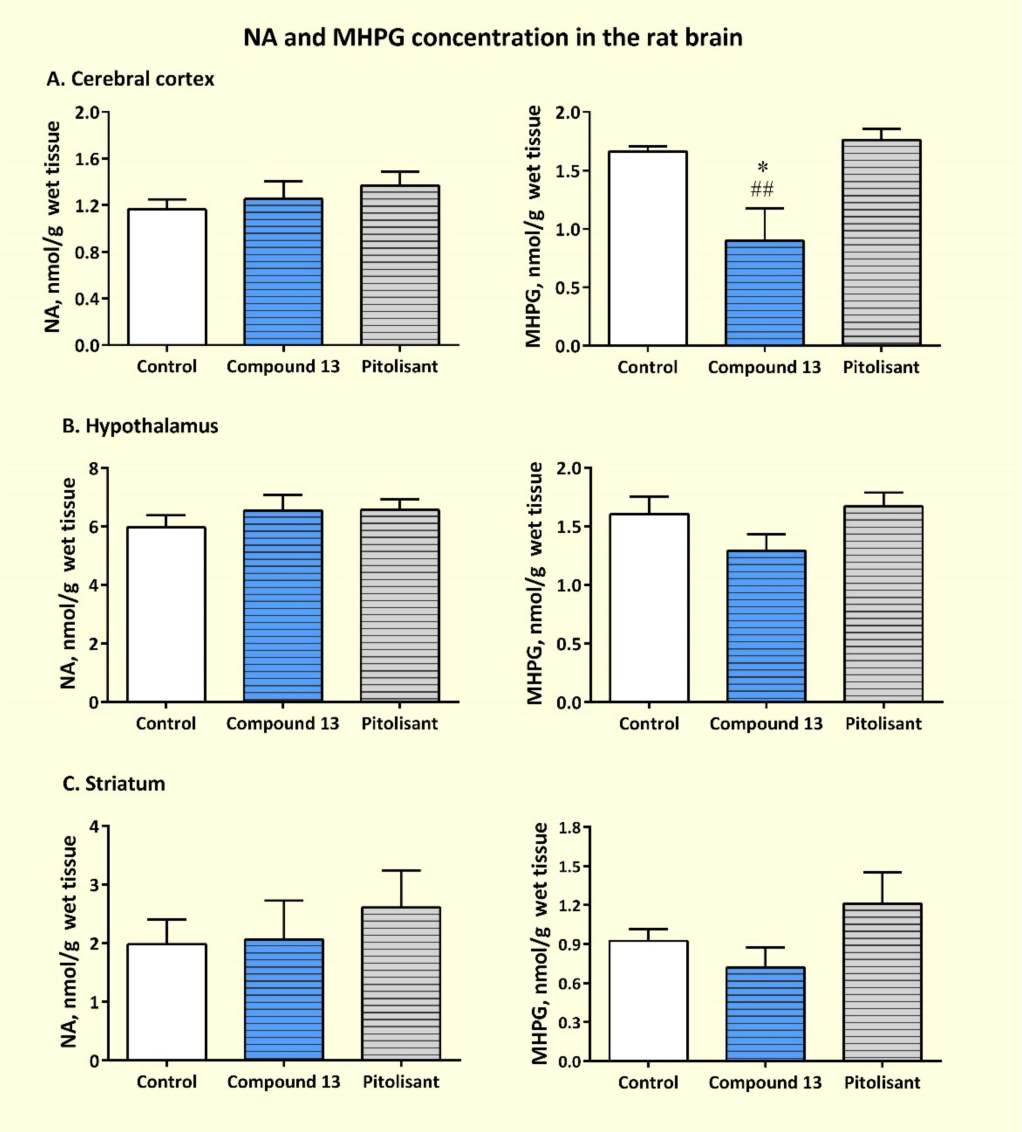

Figure 10. Concentrations of NA and MHPG in brain regions of rats sub-chronically treated with compound **13** and pitolisant (NA, noradrenaline; MHPG, 3-Methoxy-4-hydroxyphenylglycol). The drugs (both in a dose of 3 mg/kg of body mass) were injected subcutaneously for 6 consecutive days. Values are expressed as nanomoles per gram wet weight and are means ± SEM (n = 7–8). One-way ANOVA and Tukey's multiple comparisons test: * vs. control, # vs. pitolisant. One symbol means $p < 0.05$, while two symbols $p < 0.01$.

Contrary to catecholamines, sub-chronic administration of compound **13** caused a statistically significant reduction in the concentration of 5-HT and 5-HIAA in the cerebral cortex, relative to both the control and pitolisant-treated rats. HPLC analysis showed that the level of 5-HT in CTX in the compound **13** group was 1.194 ± 0.139 compared to 1.931 ± 0.167 nmol/g wet tissue in the the control group. Regarding the serotonin metabolite, 5-HIAA, the following values were obtained: 1.320 ± 0.153 and 2.246 ± 0.060 nmol/g wet tissue for the compound **13**-treated animals and control rats, respectively (Figure 11A).

In addition, there was a statistically significant decrease in the level of 5-HIAA in the hypothalamus, with no changes in 5-HT content (Figure 11B).

Compound **13** did not affect the 5-HT and 5-HIAA concentrations in the striatum (Figure 11C).

In the group of rats injected with pitolisant, post-mortem assays did not show any differences in the content in brain tissue of the examined biogenic amines nor in their metabolites compared to the control animals (Figures 9–11, Table 8).

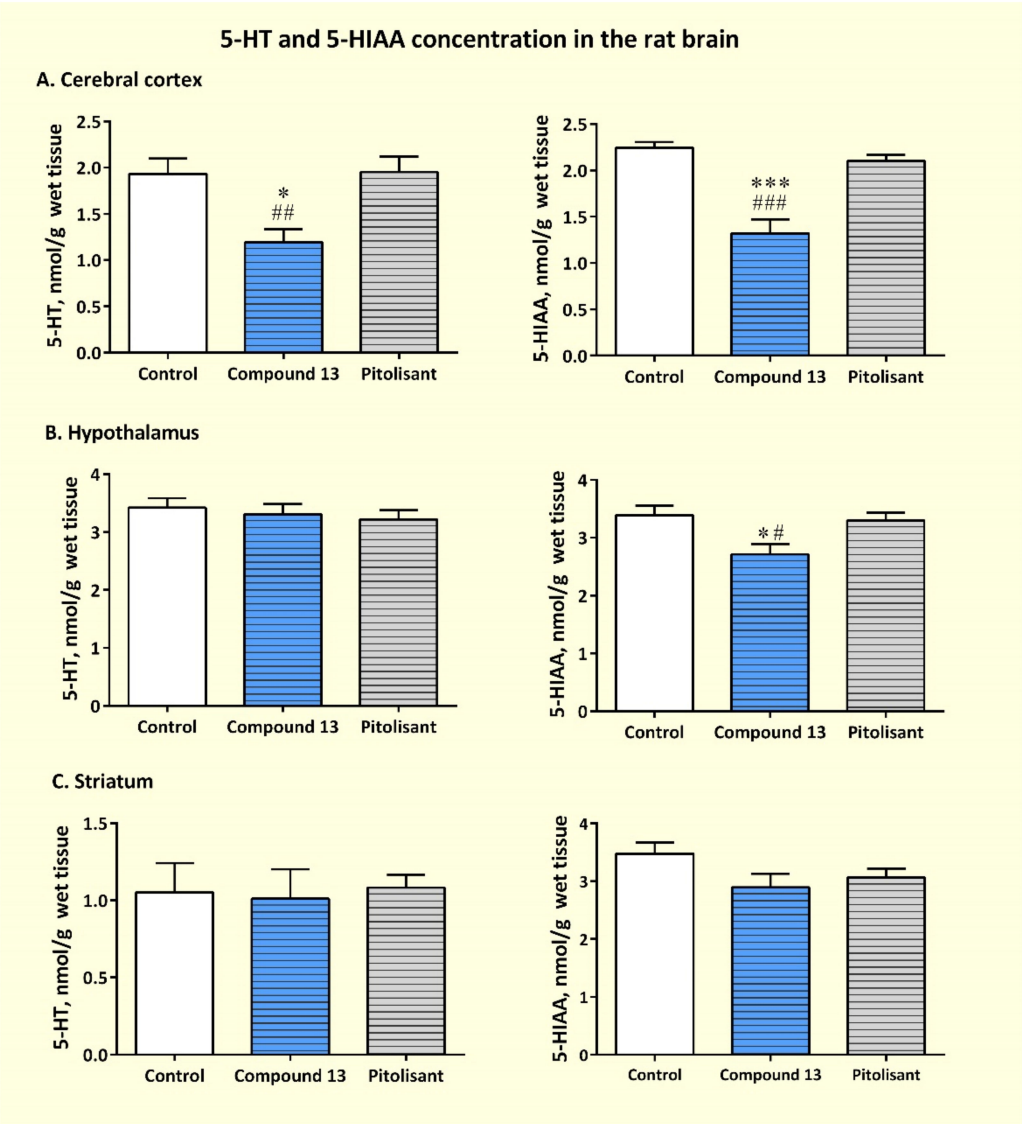

Figure 11. Concentrations of 5-HT and 5-HIAA in brain regions of rats sub-chronically treated with compound **13** and pitolisant (5-HT, serotonin; 5-HIAA, 5-hydroxyindole-3-acetic acid). The tested compounds (both in a dose of 3 mg/kg of body mass) were injected subcutaneously for 6 consecutive days. Values are expressed as nanomoles per gram wet weight and are means ± SEM (n = 7–8). One-way ANOVA and Tukey's multiple comparisons test: * vs. control, # vs. pitolisant. One symbol means $p < 0.05$, two symbols $p < 0.01$, while three symbols $p < 0.001$.

4. Discussion

According to epidemiological data, PD is the second most common neurodegenerative disorder worldwide. Inadequacies of the current pharmacotherapies to treat PD prompt efforts to identify novel drug targets. New therapeutic strategies comprise multifunctional drugs. It is assumed that drugs combining more than one activity desired in the treatment of PD will be more effective than monotherapy.

The presented research aimed to derive compounds that effectively block MAO B and show high affinity for H_3R. Continuing our previous works in this field, analogues of the compound DL76 (1-(3-(4-tert-butylphenoxy)propyl)piperidine, dual target ligand (hH_3R:

K_i = 57 nM; hMAO B IC_{50} = 48 nM) were designed and synthesized [10,11,13]. All compounds obtained were tested for affinity to hH_3R stably expressed in CHO or HEK293 cells as well as for inhibitory activity against hMAO B [6,11]. The evaluated compounds showed different activity towards both biological targets. Most of them had weak affinity for hH_3R (K_i > 500 nM), but very good inhibitory potency for hMAO B (IC_{50} < 50 nM). The most promising dual-acting ligand appeared to be 1-(3-(4-(*tert*-butyl)phenoxy)propyl)-2-methylpyrrolidine (compound **13**) (hH_3R: K_i = 25 nM; hMAO B IC_{50} = 4 nM) whereas compound **9** (3-(4-(*tert*-butyl)phenoxy)-*N*,*N*-dipropylpropan-1-amine) was the most potent hMAO B inhibitor (IC_{50} = 2 nM) with moderate affinity for hH_3R (K_i = 325 nM). Both compounds were selected for further in vitro studies. Kinetic evaluation of hMAO B inhibition showed noncompetitive and reversible behavior of both compounds. To our surprise, in the PAMPA assay, differences in penetration of the compounds through the artificial membrane were observed. compound **9** did not penetrate while compound **13** had a high penetration capacity. The permeability of a molecule across the cell membrane is an important factor determining the oral absorption and bioavailability of a drug. The lack of permeation of compound **9** is not easy to explain.

First, the experiment was repeated, as the result obtained surprised us. However, both tests gave the same result. Since the permeation of PAMPA is influenced by the chemical structure of the molecule, physicochemical parameter calculations (SwissAdme program: http://www.swissadme.ch; accessed on 22 February 2022) were performed to check this. The calculations were carried out for compound **9** and compound **13**. The results obtained, however, showed no significant differences in the values of these parameters (slightly higher logP of compound **9**—4.86 vs. 4.11 for compound **13**). One significant difference was the number of rotational bonds in the molecule (10 bonds for compound **9** and 6 bonds for compound **13**). It is known that in addition to molecular weight, the flexibility of the molecule (measured by the number of rotational bonds, polar surface area or total number of hydrogen bonds, i.e., the sum of donors and acceptors) is an important predictor of good oral bioavailability. In this case, the differences in molecular weight between compound **9** (MW = 291 g/mol) and compound **13** (MW =275 g/mol) are small, and the TPSA (12.47 Å2) and the number of hydrogen bonds (2) are the same. Thus, it is likely that the molecular flexibility of compound **9** determines its permeability, but this requires further research to confirm.

Further in vitro studies of both tested compounds (**9** and **13**) showed a dose-dependent decrease in the viability of the human astrocytes from the cerebral cortex, which was similar after 24 h and 72 h [Figure 6, Table 7]. Thus, the results of all in vitro studies allowed us to select a promising compound **13** for in vivo evaluation.

Experimental and preclinical studies performed on different animal models have convincingly shown that H_3Rs play an important role in energy balance and body weight gain and their antagonist/inverse agonists act as anorexic drugs [32–34]. Based on these reports, it was assumed that if a tested compound administered peripherally crosses the BBB, and has an antagonistic affinity for H_3Rs, it should inhibit food intake. Pitolisant, a H_3R antagonist/inverse agonist [17], was used as a reference compound. Assessment of feeding behavior in rats was performed in metabolic cages that allow precise control of daily feed and water consumption as well as urine output. As expected, in vivo studies showed that compound **13** (administered subcutaneously) crosses the BBB and inhibits feed consumption in rats to an extent similar to pitolisant (Figure 7). This observation confirms that compound **13** exhibits typical effects on feed consumption for an H_3R antagonist/inverse agonist.

In PD therapy, it is especially important to raise the cerebral DA level. MAO B inhibitors may increase DA availability in PD brain. Experimental data also suggest that MAO B inhibitors act as neuroprotective agents by decreasing the production of potentially dangerous by-products of DA metabolism in the brain [35]. In addition to symptomatic effects caused by MAO B inhibitors, it is also worth noting that (1) post-mortem analysis showed an age-related increase in MAO B activity in the human brain [36] and (2) the

enzyme is also located in the glial cells, so its enhanced activity may be a result of age-associated glial cell proliferation [35]. Thereafter, the cerebral activity of MAOs as well as concentrations of catecholamines, serotonin and their key metabolites were studied post-mortem in rats treated with compound **13**. The examined compound turned out to be a very effective MAO B inhibitor. Subcutaneous administration of it to rats for 6 days at a dose of 3 mg/kg body weight reduced MAO B activity by more than 90% (Figure 8). This is further evidence that compound **13** crosses the BBB. Post-mortem biochemical analyses in animals treated with compound **13** also showed a higher concentration of DA in the striatum and cerebral cortex (Figure 9A,C). This alteration was associated with a decrease in the concentration of DOPAC, the direct product of DA deamination by MAO B. Thus, the observed result was caused primarily by the blocking of MAO B activity by the tested compound. The correctness of this thesis was proved by a decline in DA turnover expressed as the decreased DOPAC/DA ratio (Table 8). In addition, sub-chronic injections of compound **13** caused a slight increase in NA concentration in the cerebral cortex and a statistically significant decrease in the concentration of MHPG, the final product of amine inactivation through combined deamination and methylation processes (Figure 10A). A decrease in the NA turnover was also expressed by a lower MHPG/NA ratio. It seems that the reduced MHPG concentration (and thus the lower MHPG/NA ratio value) was also a consequence of the diminishing MAOs activity. On the other hand, the tendency to increase the concentration in NA may also be partly due to a rise in DA level (its immediate precursor).

As already mentioned, the H_3R also act as heteroreceptors which modulate the release of other neurotransmitters [17,18]. At this stage of the studies, it cannot be ruled out that the increase in catecholamine levels, especially DA, may also be the result of antagonistic activity of compound **13** towards H_3R.

Surprisingly, animals treated with compound **13** had a lower concentration of serotonin (5-HT) in the cerebral cortex, relative to both the control and pitolisant-treated groups. The decrease in the level of 5-HT was also accompanied by a reduced concentration in 5-HIAA, the final amine's metabolite (Figure 11A). Turnover of 5-HT is comparable to that recorded in both other groups of rats (Table 8). The interpretation of this phenomenon requires further investigations.

Serotonin is mainly metabolized by MAO A [37,38], while administration of compound **13** lowered MAO A activity by only 12%. The concentration in 5-HT in the brain is the result of synthesis, release, reuptake, and regulation by auto- and heteroreceptors, as well as the influence of other factors that are difficult to define [39,40].

Particularly noteworthy is the 5-HT_{1A} receptor due to its key role in the autoregulation of the brain 5-HT system functional activity. Stimulation of serotonin 5-HT_{1A} receptors (5-HT_{1A}Rs) leads to reduction in the neuronal firing rate [41,42]. According to localization, the 5-HT_{1A}Rs are powerful regulators of both pre- and postsynaptic 5-HT neurotransmission. HT_{1A}Rs are found on 5-HT cell bodies and dendrites, mainly in the midbrain raphe nucleus region (presynaptically located autoreceptors) and on terminal targets of 5-HT release (postsynaptic 5-HT_{1A} receptors). 5-HT_{1A} autoreceptors inhibit neuronal spike activity in dorsal raphe nucleus and 5-HT release into the synaptic cleft [39,41]. Postsynaptic 5-HT_{1A}Rs receptors mediate the action of 5-HT on neurons and also could regulate 5-HT system functional activity via complex feedback neural networks [43,44].

In subsequent studies, we will try to verify the effect of the compound **13** on the brain's serotoninergic system, including its binding affinity for 5-HT_{1A} receptors.

5. Conclusions

Among all designed compounds, we were able to obtain compound **13**, a dual ligand, with high affinity for *h*H_3R and strong inhibition of hMAO B. The in vivo studies performed confirmed its ability to cross the BBB and showed typical effects on feed consumption for an H_3R antagonist. Moreover, compound **13** strongly inhibited brain activity of MAO B with little effect on inhibition of MAO A. Furthermore, these studies showed a positive

effect on increasing cerebral DA levels in the rat's brain. In conclusion, the results presented here predispose this compound to further experimental studies to assess its full therapeutic potential in PD.

Supplementary Materials: The following supporting information can be downloaded at https://www.mdpi.com/article/10.3390/pharmaceutics14102187/s1, Table S1 with the structures of all compounds **4**–**32** (Supplementary Materials S1); and ^{1}H and ^{13}C NMR spectra of compounds (Supplementary Materials S2).

Author Contributions: Conceptualization, D.Ł., A.S. (Anna Stasiak) and K.K.-K.; synthesis of compounds, D.Ł., W.S.-T. and E.K.; in vitro H_3R affinity studies, A.S. (Agata Siwek), D.R.-L., A.F. and H.S.; in vitro hMAO B studies, A.O.-M. and A.D.-P.; in vitro kinetic, modality and reversibility studies, A.O.-M.; in vitro PAMPA studies, E.H.-O.; assessment of cytotoxicity, A.W.-O. and M.J.-B.; HPLC analysis, M.W.; in vivo studies, A.S. (Anna Stasiak) and W.W.; biochemical analysis: A.S. (Anna Stasiak); writing—original draft preparation, D.Ł. and A.S. (Anna Stasiak); writing—review and editing, D.Ł., A.S. (Anna Stasiak), H.S. and K.K.-K.; project administration, D.Ł. and A.S. (Anna Stasiak). All authors have read and agreed to the published version of the manuscript.

Funding: This research was funded by: (1) the National Science Center grant based on decisions No. DEC 2016/23/B/NZ7/02327 (synthesis of compounds, in vitro *h*H_3R in CHO-K1 cells and hMAO B studies), (2) Jagiellonian University Medical College in Kraków grant No. N42/DBS/000300 (in vitro PAMPA assay and in vivo studies), (3) Statutory activity of Medical University of Lodz No. 503/5-087-02/ 503-51-001-19-00 (in vivo studies, assessment of cytotoxicity, HPLC analysis), (4) the EU-COST Action AC18133 (D.Ł.; D.R.-L.; H.S.; K.K.-K.), and (5) the EU-COST Action AC21115 (H.S.).

Institutional Review Board Statement: All applicable international laws for the care and use of animals were followed. The studies involving animals were performed in accordance with the ethical standards of the institution at which the studies were conducted. The animal study protocol was approved by the Local Ethical Committee for Animal Experiments in Lodz, Poland. All permits can be provided by Anna Stasiak (C-284P/2018, C-284W/2018, C-284UZ/2018; data of expiry: 29.10.2023).

Informed Consent Statement: Not applicable.

Acknowledgments: The authors would like thank Danuta Szymczak for the excellent technical assistance during the research work.

Conflicts of Interest: The authors declare no conflict of interest.

References

1. Proschak, E.; Stark, H.; Merk, D. Polypharmacology by Design: A Medicinal Chemist's Perspective on Multitargeting Compounds. *J. Med. Chem.* **2019**, *62*, 420–444. [CrossRef]
2. Ma, H.; Huang, B.; Zhang, Y. Recent advances in multitarget-directed ligands targeting G-protein-coupled receptors. *Drug. Discov. Today* **2020**, *25*, 1682–1692. [CrossRef]
3. Kuder, K.J.; Załuski, M.; Schabikowski, J.; Latacz, G.; Olejarz-Maciej, A.; Jaśko, P.; Doroz-Płonka, A.; Brockmann, A.; Müller, C.E.; Kieć-Kononowicz, K. Novel, Dual Target-Directed Annelated Xanthine Derivatives Acting on Adenosine Receptors and Monoamine Oxidase B. *ChemMedChem.* **2020**, *15*, 772–786. [CrossRef] [PubMed]
4. Affini, A.; Hagenow, S.; Zivkovic, A.; Marco-Contelles, J.; Stark, H. Novel indanone derivatives as MAO B/H_3R dual-targeting ligands for treatment of Parkinson's disease. *Eur. J. Med. Chem.* **2018**, *148*, 487–497. [CrossRef] [PubMed]
5. Lutsenko, K.; Hagenow, S.; Affini, A.; Reiner, D.; Stark, H. Rasagiline derivatives combined with histamine H_3 receptor properties. *Bioorg. Med. Chem. Lett.* **2019**, *29*, 126612. [CrossRef]
6. Łażewska, D.; Olejarz-Maciej, A.; Kaleta, M.; Bajda, M.; Siwek, A.; Karcz, T.; Doroz-Płonka, A.; Cichoń, U.; Kuder, K.; Kieć-Kononowicz, K. 4-tert-Pentylphenoxyalkyl derivatives—Histamine H_3 receptor ligands and monoamine oxidase B inhibitors. *Bioorg. Med. Chem. Lett.* **2018**, *28*, 3596–3600. [CrossRef] [PubMed]
7. Łażewska, D.; Olejarz-Maciej, A.; Reiner, D.; Kaleta, M.; Latacz, G.; Zygmunt, M.; Doroz-Płonka, A.; Karcz, T.; Frank, A.; Stark, H.; et al. Dual Target Ligands with 4-*tert*-Butylphenoxy Scaffold as Histamine H_3 Receptor Antagonists and Monoamine Oxidase B Inhibitors. *Int. J. Mol. Sci.* **2020**, *21*, 3411. [CrossRef]
8. Hagenow, S.; Stasiak, A.; Ramsay, R.R.; Stark, H. Ciproxifan, a histamine H_3 receptor antagonist, reversibly inhibits monoamine oxidase A and B. *Sci. Rep.* **2017**, *7*, 40541. [CrossRef]
9. Ligneau, X.; Morisset, S.; Tardivel-Lacombe, J.; Gbahou, F.; Ganellin, C.R.; Stark, H.; Schunack, W.; Schwartz, J.C.; Arrang, J.M. Distinct pharmacology of rat and human histamine H(3) receptors: Role of two amino acids in the third transmembrane domain. *Br. J. Pharmacol.* **2000**, *131*, 1247–1250. [CrossRef]

10. Łazewska, D.; Kieć-Kononowicz, K.; Elz, S.; Pertz, H.H.; Stark, H.; Schunack, W. Piperidine-containing histamine H3 receptor antagonists of the carbamate series: The alkyl derivatives. *Pharmazie* **2005**, *60*, 403–410.
11. Łażewska, D.; Kaleta, M.; Schwed, J.S.; Karcz, T.; Mogilski, S.; Latacz, G.; Olejarz, A.; Siwek, A.; Kubacka, M.; Lubelska, A.; et al. Biphenyloxy-alkyl-piperidine and azepane derivatives as histamine H_3 receptor ligands. *Bioorg. Med. Chem.* **2017**, *25*, 5341–5354. [CrossRef] [PubMed]
12. Cheng, Y.C.; Prusoff, W.H. Relationship between the inhibition constant (KI) and the concentration of inhibitor which causes 50 per cent inhibition (I50) of an enzymatic reaction. *Biochem. Pharmacol.* **1973**, *22*, 3099–3108. [CrossRef] [PubMed]
13. Łażewska, D.; Bajda, M.; Kaleta, M.; Zaręba, P.; Doroz-Płonka, A.; Siwek, A.; Alachkar, A.; Mogilski, S.; Saad, A.; Kuder, K.; et al. Rational design of new multitarget histamine H_3 receptor ligands as potential candidates for treatment of Alzheimer's Disease. *Eur. J. Med. Chem.* **2020**, *207*, 112743. [CrossRef] [PubMed]
14. Jóźwiak-Bębenista, M.; Sokołowska, P.; Siatkowska, M.; Panek, C.A.; Komorowski, P.; Kowalczyk, E.; Wiktorowska-Owczarek, A. The Importance of Endoplasmic Reticulum Stress as a Novel Antidepressant Drug Target and Its Potential Impact on CNS Disorders. *Pharmaceutics* **2022**, *14*, 846. [CrossRef] [PubMed]
15. Berridge, M.V.; Tan, A.S. Characterization of the cellular reduction of 3-(4,5-dimethylthiazol-2-yl)-2,5-diphenyltetrazolium bromide (MTT): Subcellular localization, substrate dependence, and involvement of mitochondrial electron transport in MTT reduction. *Arch. Biochem. Biophys.* **1993**, *303*, 474–482. [CrossRef] [PubMed]
16. Stockert, J.C.; Horobin, R.W.; Colombo, L.L.; Blázquez-Castro, A. Tetrazolium salts and formazan products in Cell Biology: Viability assessment, fluorescence imaging, and labeling perspectives. *Acta Histochem.* **2018**, *120*, 159–167. [CrossRef]
17. Schwartz, J.C. The histamine H3 receptor: From discovery to clinical trials with pitolisant. *Br. J. Pharmacol.* **2011**, *163*, 713–721. [CrossRef]
18. Gorain, B.; Sengupta, P.; Dutta, S.; Pandey, M.; Choudhury, H. Pharmacology of Histamine, Its Receptors and Antagonists in the Modulation of Physiological Functions. In *Frontiers in Pharmacology of Neurotransmitters*; Kumar, P., Deb, P.K., Eds.; Springer: Singapore, 2020; pp. 213–240. [CrossRef]
19. Stasiak, A.; Mussur, M.; Unzeta, M.; Łażewska, D.; Kieć-Kononowicz, K.; Fogel, W.A. The central histamine level in rat model of vascular dementia. *J. Physiol. Pharmacol.* **2011**, *62*, 549–558.
20. Stasiak, A.; Mussur, M.; Unzeta, M.; Samadi, A.; Marco-Contelles, J.L.; Fogel, W.A. Effects of novel monoamine oxidases and cholinesterases targeting compounds on brain neurotransmitters and behavior in rat model of vascular dementia. *Curr. Pharm. Des.* **2014**, *20*, 161–171. [CrossRef]
21. Glowinski, J.; Iversen, L.L. Regional studies of catecholamines in the rat brain. I. The disposition of [3H]norepinephrine, [3H]dopamine and [3H]dopa in various regions of the brain. *J. Neurochem.* **1966**, *13*, 655–669. [CrossRef]
22. Fowler, C.J.; Tipton, K.F. Deamination of 5-hydroxytryptamine by both forms of monoamine oxidase in the rat brain. *J. Neurochem.* **1982**, *38*, 733–736. [CrossRef]
23. Gómez, N.; Balsa, D.; Unzeta, M. A comparative study of some kinetic and molecular properties of microsomal and mitochondrial monoamine oxidase. *Biochem. Pharmacol.* **1988**, *37*, 3407–3413. [CrossRef]
24. Taylor, K.M.; Snyder, S.H. Isotopic microassay of histamine, histidine, histidine decarboxylase and histamine methyltransferase in brain tissue. *J. Neurochem.* **1972**, *19*, 1343–1358. [CrossRef] [PubMed]
25. Fogel, W.A.; Andrzejewski, W.; Maslinski, C. Brain histamine in rats with hepatic encephalopathy. *J. Neurochem.* **1991**, *56*, 38–43. [CrossRef] [PubMed]
26. Lowry, O.H.; Rosebrough, N.J.; Farr, A.L.; Randall, R.J. Protein Measurement with Folin Phenol Reagent. *J. Biol. Chem.* **1951**, *193*, 265–275. [CrossRef]
27. Kobrzycka, A.T.; Stankiewicz, A.M.; Goscik, J.; Gora, M.; Burzynska, B.; Iwanicka-Nowicka, R.; Pierzchala-Koziec, K.; Wieczorek, M. Hypothalamic NeurochemicalChanges in Long-Term RecoveredBilateral SubdiaphragmaticVagotomized Rats. *Front. Behav. Neurosci.* **2022**, *16*, 869526. [CrossRef]
28. Sander, K.; Kottke, T.; Weizel, L.; Stark, H. Kojic acid derivatives as histamine H(3) receptor ligands. *Chem. Pharm. Bull. (Tokyo)* **2010**, *58*, 1353–1361. [CrossRef]
29. Copeland, R.A. Evaluation of enzyme inhibitors in drug discovery. A guide for medicinal chemists and pharmacologists. *Methods Biochem. Anal.* **2005**, *46*, 1–265.
30. Ramsay, R.R.; Albreht, A. Kinetics, mechanism, and inhibition of monoamine oxidase. *J. Neural Transm.* **2018**, *125*, 1659–1683. [CrossRef]
31. Esbenshade, T.A.; Fox, G.B.; Cowart, M.D. Histamine H3 receptor antagonists: Preclinical promise for treating obesity and cognitive disorders. *Mol. Interv.* **2006**, *6*, 77–88. [CrossRef]
32. Guryn, R.; Staszewski, M.; Stasiak, A.; McNaught Flores, D.; Fogel, W.A.; Leurs, R.; Walczyński, K. Non-Imidazole Histamine H_3 Ligands. Part VII. Synthesis, In Vitro and In Vivo Characterization of 5-Substituted-2-thiazol-4-n-propylpiperazines. *Molecules* **2018**, *23*, 326. [CrossRef]
33. Staszewski, M.; Stasiak, A.; Karcz, T.; McNaught Flores, D.; Fogel, W.A.; Kieć-Kononowicz, K.; Leurs, R.; Walczyński, K. Design, synthesis, and in vitro and in vivo characterization of 1-{4-[4-(substituted)piperazin-1-yl]butyl}guanidines and their piperidine analogues as histamine H_3 receptor antagonists. *MedChemComm* **2019**, *10*, 234–251. [CrossRef] [PubMed]
34. Provensi, G.; Blandina, P.; Passani, M.B. The histaminergic system as a target for the prevention of obesity and metabolic syndrome. *Neuropharmacology* **2016**, *106*, 3–12. [CrossRef]

35. Schapira, A.H.V. Monoamine Oxidase B Inhibitors for the Treatment of Parkinson's Disease. *CNS Drugs* **2011**, *25*, 1061–1071. [CrossRef]
36. Fowler, J.S.; Volkow, N.D.; Wang, G.J.; Logan, J.; Pappas, N.; Shea, C.; MacGregor, R. Age-related increases in brain monoamine oxidase B in living healthy human subjects. *Neurobiol. Aging* **1997**, *18*, 431–435. [CrossRef]
37. Tan, Y.Y.; Jenner, P.; Chen, S.D. Monoamine Oxidase-B Inhibitors for the Treatment of Parkinson's Disease: Past, Present, and Future. *J. Parkinsons Dis.* **2022**, *12*, 477–493. [CrossRef] [PubMed]
38. Youdim, M.B.; Bakhle, Y.S. Monoamine oxidase: Isoforms and inhibitors in Parkinson's disease and depressive illness. *Br. J. Pharmacol.* **2006**, *147*, S287–S296. [CrossRef] [PubMed]
39. Pytliak, M.; Vargová, V.; Mechírová, V.; Felšöci, M. Serotonin receptors—From molecular biology to clinical applications. *Physiol. Res.* **2011**, *60*, 15–25. [CrossRef]
40. McCorvy, J.D.; Roth, B.L. Structure and function of serotonin G protein-coupled receptors. *Pharmacol. Ther.* **2015**, *150*, 129–142. [CrossRef]
41. You, I.J.; Wright, S.R.; Garcia-Garcia, A.L.; Tapper, A.R.; Gardner, P.D.; Koob, G.F.; Leonardo, E.D.; Bohn, L.M.; Wee, S. 5-HT1A Autoreceptors in the Dorsal Raphe Nucleus Convey Vulnerability to Compulsive Cocaine Seeking. *Neuropsychopharmacology* **2016**, *41*, 1210–1222. [CrossRef] [PubMed]
42. Andrade, R.; Huereca, D.; Lyons, J.G.; Andrade, E.M.; McGregor, K.M. 5-HT1A Receptor-Mediated Autoinhibition and the Control of Serotonergic Cell Firing. *ACS Chem. Neurosci.* **2015**, *6*, 1110–1115. [CrossRef]
43. Sharp, T.; Boothman, L.; Raley, J.; Queree, P. Important messages in the 'post': Recent discoveries in 5-HT 707 neurone feedback control. *Trends Pharmacol. Sci.* **2007**, *28*, 629–636. [CrossRef] [PubMed]
44. Altieri, S.C.; Garcia-Garcia, A.L.; Leonardo, E.D.; Andrews, A.M. Rethinking 5-HT1A receptors: Emerging modes of inhibitory feedback of relevance to emotion-related behavior. *ACS Chem. Neurosci.* **2013**, *4*, 72–83. [CrossRef] [PubMed]